

Fall 2004

# Obtaining optimal data length for FMRI images

Vikram M. Natarajan  
*New Jersey Institute of Technology*

Follow this and additional works at: <https://digitalcommons.njit.edu/theses>



Part of the [Biomedical Engineering and Bioengineering Commons](#)

---

## Recommended Citation

Natarajan, Vikram M., "Obtaining optimal data length for FMRI images" (2004). *Theses*. 466.  
<https://digitalcommons.njit.edu/theses/466>

This Thesis is brought to you for free and open access by the Theses and Dissertations at Digital Commons @ NJIT. It has been accepted for inclusion in Theses by an authorized administrator of Digital Commons @ NJIT. For more information, please contact [digitalcommons@njit.edu](mailto:digitalcommons@njit.edu).

## Copyright Warning & Restrictions

The copyright law of the United States (Title 17, United States Code) governs the making of photocopies or other reproductions of copyrighted material.

Under certain conditions specified in the law, libraries and archives are authorized to furnish a photocopy or other reproduction. One of these specified conditions is that the photocopy or reproduction is not to be “used for any purpose other than private study, scholarship, or research.” If a user makes a request for, or later uses, a photocopy or reproduction for purposes in excess of “fair use” that user may be liable for copyright infringement,

This institution reserves the right to refuse to accept a copying order if, in its judgment, fulfillment of the order would involve violation of copyright law.

**Please Note: The author retains the copyright while the New Jersey Institute of Technology reserves the right to distribute this thesis or dissertation**

Printing note: If you do not wish to print this page, then select “Pages from: first page # to: last page #” on the print dialog screen



The Van Houten library has removed some of the personal information and all signatures from the approval page and biographical sketches of theses and dissertations in order to protect the identity of NJIT graduates and faculty.

## **ABSTRACT**

### **OBTAINING OPTIMAL DATA LENGTH FOR FMRI IMAGES**

**by  
Vikram M. Natarajan**

Interest in brain hemodynamics has led to a substantial increase in state of the art research within the field of functional Magnetic Resonance Imaging (fMRI). FMRI enables research to be conducted on brain mapping in healthy individuals, as well as in patient populations. The need for accurate functional images is required. The primary objective was the development of a method to determine the optimal number of time points required to obtain reliable activation maps. The second phase involved the development of a program, which enabled the conversion of functional magnetic resonance images to a format that the neurosurgeon's scanner could read. Obtaining an accurate functional activation map by reducing the number of time points, in addition to converting it to a format which allows the surgeon to view the images in real-time on his scanner during stereo-tactic surgery will increase the success rate in brain surgery.

**OBTAINING OPTIMAL DATA LENGTH  
FOR FMRI IMAGES**

by  
**Vikram M. Natarajan**

**A Thesis  
Submitted to the Faculty of  
New Jersey Institute of Technology  
in Partial Fulfillment of the Requirements for the Degree of  
Master of Science in Biomedical Engineering**

**Department of Biomedical Engineering**

**January 2005**

Blank Page

**APPROVAL PAGE**  
**OBTAINING OPTIMAL DATA LENGTH**  
**FOR FMRI IMAGES**

**Vikram M. Natarajan**

---

Dr. Bharat B. Biswal, Thesis Advisor Date  
Associate Professor of Department of Radiology, UMDNJ

---

Dr. Stanley Reisman, Thesis Co-Advisor Date  
Professor of Biomedical Engineering, NJIT

---

Dr. Tara Alvarez, Committee Member Date  
Assistant Professor of Biomedical Engineering, NJIT

## **BIOGRAPHICAL SKETCH**

**Author:** Vikram M. Natarajan

**Degree:** Master of Science

**Date:** January 2005

### **Undergraduate and Graduate Education:**

- Master of Science in Biomedical Engineering,  
New Jersey Institute of Technology, Newark, NJ, 2005
- Bachelor of Science in Electrical Engineering,  
New Jersey Institute of Technology, Newark, NJ, 2003

**Major:** Biomedical Engineering

### **Presentations and Publications:**

Vikram M. Natarajan and Dr. Bharat B. Biswal,  
“Obtaining Optimal Data Length for FMRI Images,”  
The Thirteenth Scientific Meeting & Exhibition (ISMRM'05), South Beach,  
Miami, Florida, May 2005.



**Affectionately dedicated to my loving and caring parents**

## **ACKNOWLEDGMENT**

My sincere thanks to my mentor, Dr. Bharat B. Biswal who guided me on this project with his invaluable assistance at all times including weekends and holidays. My special thanks to Dr. Stanley Reisman, and Dr. Tara Alvarez for actively participating in my committee. My many thanks to Ms. Stella Dixon Brown, and Ms. Pawan Singh for making time to scan many of my subjects.

## TABLE OF CONTENTS

<b>Chapter</b>	<b>Page</b>
1 INTRODUCTION .....	1
1.1 Objective .....	1
1.2 Overview .....	1
2 MAGNETIC RESONANCE IMAGING (MRI) .....	4
2.1 History of MRI .....	4
2.2 Physics of MRI .....	4
2.3 Image Contrast and Enhancement .....	6
2.4 Relaxation Times .....	6
2.4.1 T1 Relaxation .....	7
2.4.2 T2 Relaxation .....	8
2.5 Weighted Images T2/T2 .....	9
2.6 Echo Planar Imaging (EPI) .....	10
3 FUNCTIONAL MAGNETIC RESONANCE IMAGING (fMRI) .....	13
3.1 Introduction .....	13
3.2 Analyzing the BOLD Signal .....	14
3.3 How Tasks are Presented to the Subject/Patient .....	16
3.4 Using fMRI to Perform Surgery .....	18
3.4.1 Brain Mapping .....	18
3.4.2 Stereo-tactic Surgery .....	19
3.4.3 Possible Complications .....	20

**TABLE OF CONTENTS**  
**(Continued)**

<b>Chapter</b>	<b>Page</b>
4 DATA ANALYSIS METHODS .....	22
4.1 Introduction .....	22
4.2 Motion Correction .....	22
4.3 Separating True Activation from Noise .....	24
4.4 The t-test .....	25
4.5 Correlation Analysis .....	26
4.6 Fourier Imaging .....	28
4.7 The Kolmogorov-Smirnov Test .....	31
4.8 Noise Correlations .....	32
4.9 Reliability of Activation .....	32
5 THE EXPERIMENT .....	34
5.1 Introduction .....	34
5.2 Steps taken to Scan a Subject and Analyze the Data .....	36
5.3 Motion Corrected Data .....	39
5.4 Determining Optimal Data Length for fMRI Images .....	44
5.5 Results .....	52
6 DEVELOPMENT OF FILE CONVERSION SOFTWARE .....	53
7 DISCUSSION .....	58
APPENDIX A SCRIPT FILE WRITTEN TO GENERATE MEAN AND STANDARD DEVIATION FOR MOTION CORRECTED DATA ...	62

**TABLE OF CONTENTS**  
**(Continued)**

<b>Chapter</b>	<b>Page</b>
APPENDIX B PROGRAM USED TO RECONSTRUCT RAW DATA FROM MRI SCANNER .....	64
APPENDIX C SCRIPT FILE WRITTEN TO CONVERT FILE FORMAT .....	65
REFERENCES .....	67

## LIST OF TABLES

<b>Table</b>		<b>Page</b>
2.1	Water Content in Human Tissue .....	6
5.1	Motion Corrected Data for Subject # 1 .....	40
5.2	Motion Corrected Data for Subject # 2 .....	41
5.3	Motion Corrected Data for Subject # 3 .....	41
5.4	Motion Corrected Data for Subject # 4 .....	41
5.5	Motion Corrected Data for Subject # 5 .....	42
5.6	Motion Corrected Data for Subject # 6 .....	42
5.7	Motion Corrected Data for Subject # 7 .....	42
5.8a	Motion Corrected Data for Subject # 8 (Session 1) .....	43
5.8b	Motion Corrected Data for Subject # 8 (Session 2) .....	43
5.9	Optimal Number of Time Points for each Subject Scanned .....	52

## LIST OF FIGURES

<b>Figure</b>	<b>Page</b>
2.1 Basic Idea of NMR Imaging .....	5
2.2 T1 Relaxation Curve .....	7
2.3 T2 Relaxation Curve .....	9
2.4a T1 Weighted Image .....	10
2.4b T2 Weighted Image .....	10
2.5 Echo Planar Imaging .....	11
3.1 The BOLD Signal .....	15
3.2 MRI Image Showing Brain Tumor .....	17
3.3 fMRI Image Obtained During Finger Tapping Paradigm .....	17
4.1 fMRI Image Obtained Using Cross-Correlation .....	27
4.2 BOLD Signal Obtained From Text Listening Paradigm .....	28
4.3 Fourier Components of the BOLD Signal .....	29
5.1 Sagittal View of Motor Cortex .....	35
5.2 Axial View of Motor Cortex .....	35
5.3 Axial View of Wernicke's Area .....	36
5.4 Stimulus Paradigm .....	38
5.5a fMRI Image Obtained from a Finger Tapping Paradigm Before Motion Correction .....	43
5.5b fMRI Image after Motion Correction .....	43
5.6a Images Obtained by Varying Number of Time Points from 15 – 55 during a Text Listening Paradigm .....	46

**LIST OF FIGURES  
(Continued)**

<b>Figure</b>	<b>Page</b>
5.6b Images Obtained by Varying Number of Time Points from 60 – 90 during a Text Listening Paradigm .....	47
5.7a Legend Used for Figures 5.7b, c, and d .....	48
5.7b Number of Activated Voxels from Silent Word Generation Paradigm .....	49
5.7c Number of Activated Voxels from Text Listening Paradigm .....	49
5.7d Number of Activated Voxels from Finger Tapping Paradigm .....	49
5.8a Images Obtained by Varying Number of Time Points from 15 – 55 during a Finger Tapping Paradigm .....	50
5.8b Images Obtained by Varying Number of Time Points from 60 – 90 during a Finger Tapping Paradigm .....	51
6.1 FMRI Image Used in File Conversion Program .....	54
6.2 Image Properties Obtained from Figure 6.1 .....	55
6.3 Image Obtained after Conversion to Dicom Format .....	56
6.4 Image Properties Obtained from Figure 6.3 .....	57



# **CHAPTER 1**

## **INTRODUCTION**

### **1.1 Objective**

An arbitrary number of sequential images are obtained while the subject performs assigned tasks. Statistical methods are then used to detect and localize brain activation. Data analyzed using a minimal number of time points yields unreliable data due to a lack of statistical power. A collection of long sequential data with sufficient statistical power may still provide unreliable information. As time progresses, movement becomes more prevalent. Also, habituation, adapting to the task/paradigm, might occur. These two reasons make long time series potentially faulty. Essentially, enough data must be compiled that will provide accurate information, without providing an excess of unreliable data. This is particularly relevant in patient populations, where the subject might not be able to perform the task for a long time due to a variety of neuro-psychiatric illnesses such as traumatic brain injury, stroke, brain tumors, Alzheimer's disease, Schizophrenia, etc. The optimal use of the number of sequential images is important in order to stay efficient, accurate, and timely. In this study, a technique was devised to determine the optimal number of time points required to obtain reliable activation maps.

### **1.2 Overview**

Magnetic Resonance Imaging (MRI) uses radio waves as well as a strong magnetic field rather than x-rays to provide clear, detailed pictures of internal organs and tissues. FMRI is a relatively new procedure that uses MR imaging to measure metabolic changes that

take place in different regions of the brain. Physicians are aware of the general regions of the brain where speech, sensation, memory, and other functions originate; however, the exact locations vary from individual to individual. Injuries and diseases, such as stroke or brain tumor, can cause functions to shift to other regions of the brain. FMRI not only assists radiologists, and researchers to scrutinize (with greater temporal and spatial resolution) the anatomy of the brain, but can also facilitate in precisely determining and localizing the region of the brain related to some of the critical functions such as thought, memory, speech, movement, and sensation. This information can be critical in planning surgery, radiation therapy, treatment for stroke, or other interventions to treat brain disorders. [6]

Removing a brain tumor is a complex procedure. A surgeon's desire to excise a tumor (bad tissue) does not overshadow the need to leave good, healthy, functional tissue surrounding the tumor undisturbed. Damaging functional, healthy tissue might cause severe, irreversible disability in a person. Once the location of the tumor is determined, the surgeon would be interested in the extent and degree of function of the healthy tissues surrounding the tumor. Most of the time, the tissue surrounding the tumor is used for certain tasks such as sensory, motor, speech, listening, vision, etc.

FMRI is used to determine which regions of the brain are being used for certain tasks and is becoming the diagnostic method of choice for studying brain function in a normal, diseased or injured subject. FMRI can also be used serially to assess brain function over time, as well as to study altering brain function following an invasive treatment.

In routine practice, fMRI studies are used in planning brain surgery, because they aid physicians to monitor and visualize normal as well as altered brain function. This will show regions of activation in interested areas of the brain. The main problem is obtaining accurate activation maps that can be used during stereo-tactic brain surgery. In order for accurate activation maps to be obtained, the subject must lie in the MRI machine, and avoid any movement while the scan is being performed, which is unachievable at this time. Head motion due to swallowing, sneezing, etc. always yields results, which are difficult to interpret without using image processing methods (i.e. motion registration, cross-correlation, Fourier Imaging, etc.) to eliminate noise. For this reason, the innovative method discussed in this document was developed. The method used cross-correlation to obtain reliable activation maps, by varying the number of time points. The images obtained through this procedure can be used during brain surgery for the removal of tumors, and will reduce the number of surgical errors.

## **CHAPTER 2**

### **MAGNETIC RESONANCE IMAGING (MRI)**

#### **2.1 History of MRI**

The first successful demonstrations of Nuclear Magnetic Resonance (NMR) in bulk matter were published in 1946. Two independent groups, unknown to each other, working in physics laboratories on opposite coasts of the United States, discovered NMR almost simultaneously. Bloch, Hansen, and Packard, working at Stanford University, and Purcell, Torrey, and Pound, working at Harvard University, published their results in consecutive issues of *The Physical Review*. [28]

The impact of their work was immediate, and the applications of NMR have widened steadily from physics and chemistry to a surprising range of disciplines from archeology to medicine. The importance of the discovery was recognized by the joint award to the 1952 Nobel Prize for Physics to the two leaders, Professor Felix Bloch and Professor Edward Purcell. [16]

#### **2.2 Physics of MRI**

MR imaging takes advantage of the magnetic moments of nuclei associated with their spin. The force acting on a nuclear moment  $\mu$  placed in a magnetic field  $\mathbf{B}$  is the basic interaction that leads to NMR. In addition to the magnetic moment, the nuclei possess an angular momentum. This can be visualized as gyroscopes that precess under the influence of the applied magnetic field with the angular velocity about the magnetic field (shown in equation 2.1). [16]

$$\Omega = -\gamma \cdot \mathbf{B} \quad (2.1)$$

MR imaging relies on the use of magnetic field gradients to disperse the MR frequencies of the various volume elements of a medical project. The basic idea of MR imaging is illustrated in figure 2.1. In figure 2.1 a linear magnetic field gradient applied along an axis of the object leads to resonance frequencies characteristic of the position along this axis. All the volume elements in a plane perpendicular to this axis exhibit similar resonance frequencies, and contribute to the same signal amplitude. Hence, the MR spectrum can be considered as a one-dimensional projection of the three-dimensional density of the observed nuclear spin species onto the direction of the field gradient. [16]

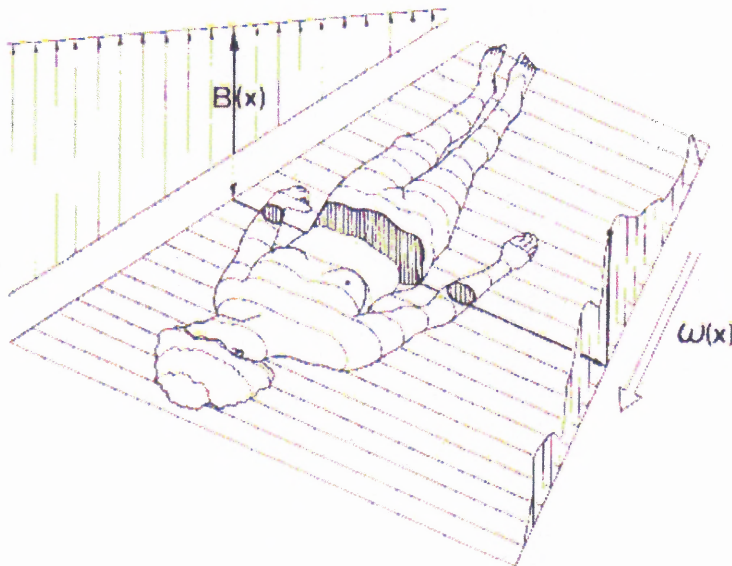


**Figure 2.1** Basic Idea of NMR Imaging. The NMR signal is recorded in the presence of a linear magnetic field gradient  $\mathbf{B}(x)$ . It is recorded such that the resonance frequency  $\omega$  is a linear function of the spatial coordinate  $x$ . [16]

### 2.3 Image Contrast and Enhancement

The parameters that govern signal intensity in each volume element (voxel) in an MR image are T1 and T2, the longitudinal and transverse relaxation times of the water protons in the tissue. In a strong magnetic field, the water protons are excited when they absorb energy in the radio frequency range. Table 2.1 shows the percent of water content in each type of human tissue. In practice, the energy is offered as a microsecond pulse from an RF coil. When the pulse is turned off, the protons return to their original equilibrium state. The return process is known as relaxation and is a much slower process than RF absorption (approximately one second difference). The relaxation process is assumed to be of the first-order. The rate of progress toward equilibrium is proportional to the deviation from equilibrium. [16]

**Table 2.1** Water Content in Human Tissue

<b>Tissue</b>	<b>Water Content (%)</b>
Gray Matter	70.6
White Matter	84.3
Heart	80.3
Blood	93.0
Bone	12.2

### 2.4 Relaxation Times

The processes determining the return to equilibrium to both longitudinal and transverse magnetization are summarized by the term relaxation. These two processes are the key factors in distinguishing tissues in MR images. Before imaging, a decision must be made as to the type of information one is attempting to gain from the examination. Signal intensity of MR images is a function of T1, T2, and proton density. [16]

### 2.4.1 T1 Relaxation

The return of excited nuclei from a high energy state to a low energy or ground state is associated with the loss of energy to the surrounding nuclei. NMR was originally used to examine solids in the form of lattices. This is how the name spin-lattice relaxation was created. T1 relaxation is characterized by the longitudinal return of the net magnetization to its ground state of maximum length in the direction of the main magnetic field. The rate of return is an exponential process as is shown in figure 2.2. Equation 2.2 shows the equation behind T1 relaxation. [2]

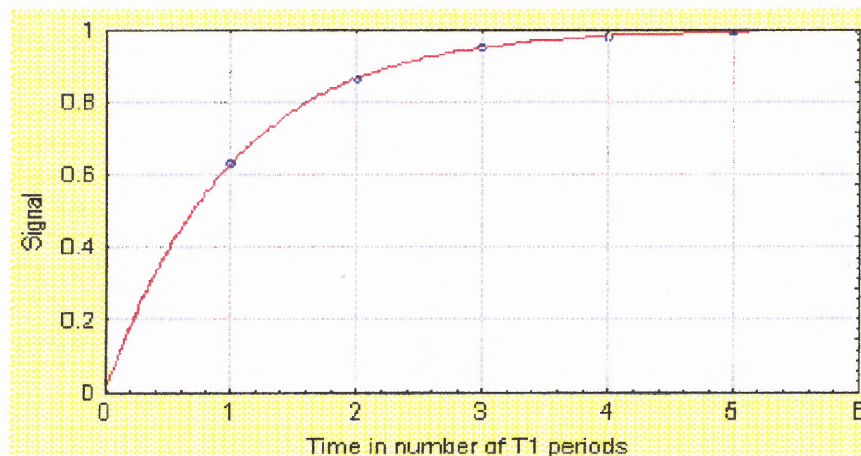


**Figure 2.2** T1 Relaxation Curve. [2]

$$M = M_0 \cdot (1 - e^{-t/T1}) \quad (2.2)$$

The T1 relaxation time is the time required for the magnetization to return to 63% of its original length. After two T1 cycles, the magnetization is at 86% of its original length. After three T1 times the result is 95% of the original length. Spins are

considered completely relaxed after approximately 3 to 5 T1 times. Another term that is commonly used is R1 relaxation rate. This is the reciprocal of the T1 time ( $1/T1$ ). [2]

Given similar proton densities, tissues with a short T1 have a brighter (whiter) representation of the image. Tissues with a long T2 are indicated by a whiter (more intense) image. In order to bring out differences in T1, shorter TR's (repetition time) of approximately 250 ms should be used. Tissues with a short T1 time (250 ms) will yield high signal intensity, since their protons have returned to their maximum longitudinal relaxation between imaging pulses. Those with long T1 (1sec to 2 sec) will not have relaxed completely before the next pulse and consequently will become partially saturated. They will give off a less intense signal with subsequent pulses, thereby allowing differentiation from rapidly relaxing tissues. [16]

#### **2.4.2 T2 Relaxation**

T2 relaxation or spin-spin relaxation occurs (microscopically) when spins in the high and low energy state exchange energy, but do not lose energy to the surrounding lattice. This results macroscopically in loss of the transverse magnetization. In pure water, the T2 and T1 times are approximately the same, which is approximately 2 to 3 seconds. However, in biological materials, the T2 time is significantly shorter than the T1 time. For brain white matter,  $T1=0.5$  seconds and  $T2=0.07$  seconds (70 msec). T2 relaxation occurs exponentially like T1 relaxation with 63% of the transverse magnetization dissipated after one T2 period as shown in figure 2.3. The equation governing T2 relaxation is shown in equation 2.3.



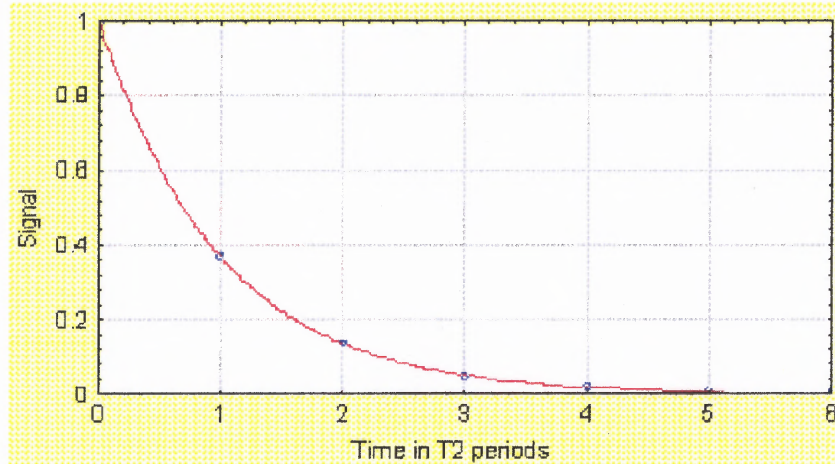


**Figure 2.3** T2 Relaxation Curve. [2]

$$M = M_0 \cdot e^{(-t/T2)} \quad (2.3)$$

T2 relaxation is, much shorter than T1 relaxation, so the differences in T2 are not well demonstrated by a change in TR. Alternation in the echo time (TE), by increments of 30 ms (30, 60, 90, 120 ms TE's) will enhance the differences in T2 relaxation present within the tissues. A tissue with a long T2 should become brighter on the later echoes at a given TR. Unfortunately, increasing T2, decreasing T1, and increasing proton density may work antagonistically in the final image to mask a lesion. [16]

### 2.5 Weighted Images T1/T2

MRI has become an indispensable tool in diagnostic radiology. MRI clearly shows researchers fine details of anatomy, and yet is noninvasive and does not require ionizing radiation such as x-rays. MRI is a highly flexible technique so that contrast between one tissue and another in an image can be varied simply by varying the way the image is made. Figure 2.4a and b show two magnetic resonance (MR) images of the same

anatomical section, illustrating completely different patterns of contrast. These two images are described as T1-weighted, and T2-weighted, respectively. The source of the flexibility of MRI is the fact that the measured signal depends on many properties of the tissue. This is clearly illustrated in figure 2.4. [4]

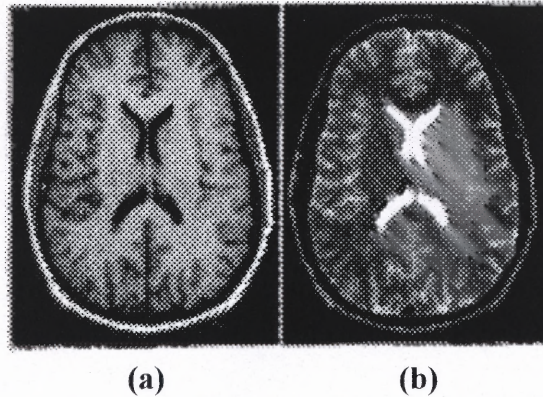


**Figure 2.4** (a) T1 Weighted Image. TR = 600, TE = 11 (b) T2 Weighted Image. TR = 3800, TE = 102. The contrast is altered during image acquisition by adjusting several parameters. [4]

In addition to the advantages of MRI, there are also downsides. Some downsides include the inability to image certain individuals that have implants, braces, or even bullets in their body. When scanning these types of individuals many artifacts are present in the images obtained.

## 2.6 Echo Planar Imaging (EPI)

The most common imaging technique for fMRI is single shot EPI. The idea of echo planar imaging was proposed early in the history of MRI, but it is only in the last few years that this technique has become widely available. Figure 2.5 shows a simplified pulse sequence diagram for a single shot (EPI) pulse sequence. The boxed region of the

EPI pulse sequence is shown in figure 2.5. It is repeated  $N/2$ , where  $N$  is the total number of lines measured in k-space. [19]

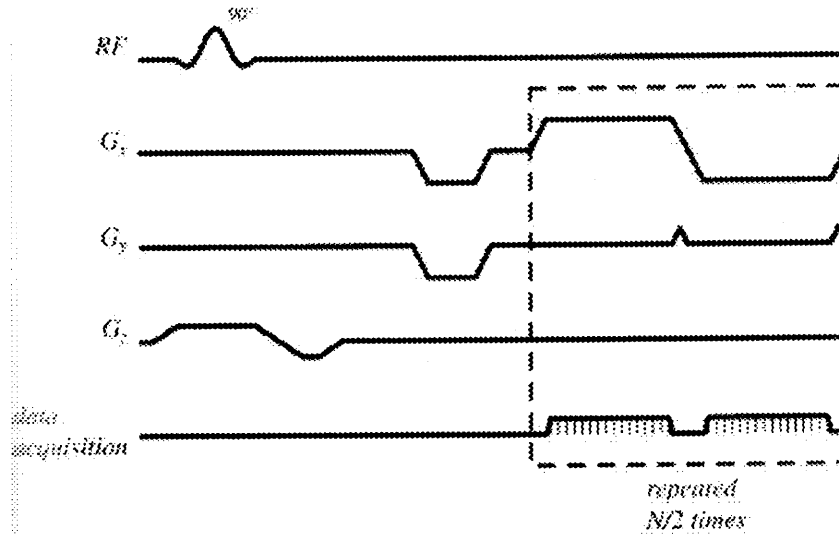


**Figure 2.5** Echo Planar Imaging. The pulse sequence diagram illustrates the rapidly switched gradient pulses, which is used for a back and forth scanning of k-space. [19]

EPI requires strong gradients and rapid switching capabilities. A central problem in using single-shot imaging is that the data acquisition window is limited by  $T2^*$ . ( $T2^*$  is the time constant for the loss of phase coherence among spins oriented at an angle to the static magnetic field. This is due to a combination of magnetic field inhomogeneities and the spin-spin relaxation.  $T2^*$  results in a rapid loss of transverse magnetization (faster than  $T2$ ) as well loss of MRI signal.) The intrinsic signal will have significantly decayed during data acquisition. The corresponding k-space samples are often larger k samples describing the high spatial frequencies. This amounts to an additional blurring of the image. [4]

Spatial resolution in single-shot EPI is limited either by the area of k-space that can be critically sampled in approximately one  $T2^*$  period or by the system bandwidth. The area of k space that can be covered can be limited by the velocity in k space (gradient amplitude) of the acceleration in k space, (gradient slew rate) and is typically limited by both. The tradeoff between gradient amplitude and gradient slew rate in design of the gradient system is one that has application-specific optima. Systems that are designed specifically for single-shot EPI generally perform this function most efficiently. [19]

The requirement for strong and rapidly switching gradients can be satisfied by increasing the gradient amplifier power, implementing resonant gradient technology, or by reducing the inductance of the gradient coils such that they can be driven by conventional gradient amplifiers. [19]

## CHAPTER 3

### FUNCTIONAL MAGNETIC RESONANCE IMAGING (fMRI)

#### 3.1 Introduction

fMRI is used to determine brain function, by detecting changes in the chemical composition of brain areas or changes in the flow of fluids that occur over time spans of seconds to sometimes minutes. This method can also be used to study the physiology of various organs including the brain. In the brain, blood perfusion is related to neural activity, so fMRI, like other imaging techniques such as PET, and SPECT, can be used to localize distinct brain regions corresponding to specific tasks or specific stimuli. [4]

In recent years, fMRI has created a revolution in research on the basic function of the healthy human brain. When neural activity increases in a region of the brain while the subject performs certain tasks/stimulus, the local MR signal produced in that part of the brain increases by a small amount due to the changes in blood oxygenation. This Blood Oxygenation Level Dependent (BOLD) effect is the basis for most of the fMRI studies currently performed. These studies are done to map patterns of activation in the working human brain. [4]

The BOLD effect is most evident on gradient echo (GRE) images, which indicate that the effect is primarily an increase of the local value of  $T2^*$ . The fact that the oxygenation of the blood has a measurable effect on the MR signal from the surrounding tissue was discovered by Ogawa and co-workers imaging a rat model at 7T. [4] They discovered that the MR signal around the veins decrease when the oxygen content of the inspired air was reduced. The effect was reversed when the oxygen content was returned

to normal values. The oxygen sensitivity of the MR signal from blood was known from previous studies, which showed that T2 depended strongly on the oxygenation of hemoglobin. In this study, the researchers also observed that the signal reductions were not just in the blood itself, but also in the tissue space around the vessels. This suggested that T2\* was reduced in the intravascular and extravascular spaces. [4]

All these early physiological manipulations demonstrated that reductions in blood oxygenation led to a signal decrease. Kwong [4] demonstrated that brain activation in human subjects produced a local signal increase that could be used for functional brain mapping. In addition, several other groups reported similar findings. [4] The discovery that activation produced a signal increase was somewhat surprising because it indicated that the T2\* had increased, rather than decreased. This was surprising because it suggested that blood was more oxygenated with activation.

### **3.2 Analyzing the BOLD Signal**

The use of BOLD contrast for the observation of brain activation was first demonstrated in August of 1991 at the 10<sup>th</sup> Annual Meeting of the Society of Magnetic Resonance in Medicine [19]. The first papers demonstrating the technique were published in July 1992. They essentially showed human brain activation in the primary visual cortex and motor cortex. Two of the first three reports of this technique involved the use of EPI. In these experiments a small significant local signal increase in the activated cortical regions was observed using susceptibility-weighted, gradient-echo pulse sequence. [19]

fMRI, based on the blood oxygenation level dependent has become a widely used tool for probing the working brain. The goal of fMRI studies is to map patterns of local

changes in the magnetic resonance signal in the brain as an indicator of neural activity associated with particular stimuli. The prototypical fMRI experiment alternates blocks of stimulus and control periods while a series of dynamic images is collected with an echo-planar imaging (EPI) pulse sequence. The signal time course for each voxel of the image is analyzed to test whether there is a significant correlation of the signal with the stimulus (i.e., whether the signal increased during stimulus). [4]

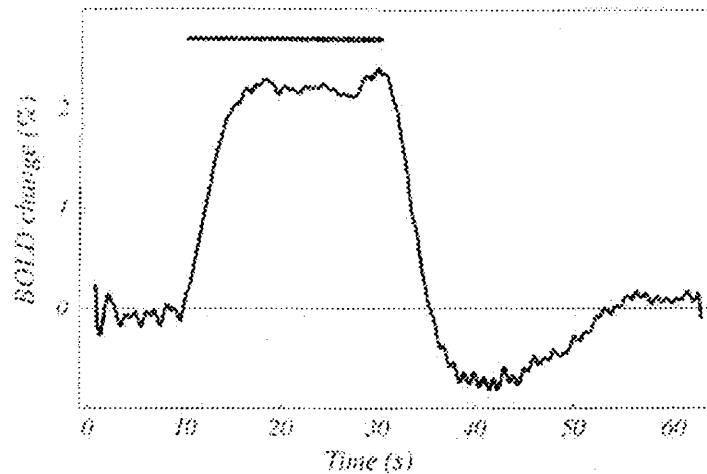


**Figure 3.1** The BOLD Signal. Sample BOLD response in the visual cortex measured at 3T. [4]

Figure 3.1 clearly shows an example of the BOLD signal response in the visual cortex during a simple visual stimulus. This is a typical method to view activation in the brain. The dynamic MR images provided a time course for the signal from each voxel, and those voxels showing a significant correlation with the stimulus pattern were selected and averaged to form the time course shown in figure 3.1. Figure 3 was obtained by averaging data obtained from three subjects during a simple visual stimulus. [4]

The average response in figure 3.1 is fairly typical of BOLD responses to a number of stimuli. Similar results are obtained for tasks such as bilateral finger tapping, silent word generation, and text listening. There is an initial delay of approximately 1 to 3 seconds which is due to the time it takes for the subject to comprehend the instructions and actually start the task. Followed by this is a ramp of 5 to 8 seconds, just before a plateau signal is reached. After the end of the stimulus, the BOLD signal ramps down over several seconds and often undershoots the original baseline. This undershoot typically takes 20 seconds to return to the baseline, which is clearly shown in figure 3.1. The BOLD signal may vary from subject to subject depending on the task or age. For example if a memory task is presented to the subject, testing younger age groups would yield better results.

### **3.3 How Tasks are Presented to the Subject/Patient**

Functional MRI is used for basic science as well as on clinical patient populations. When used for research, the intended goal is to understand brain function. Clinical patients on the other hand are scanned for specific reasons. When a tumor is located, (i.e figure 3.2) it must be removed. Depending on the location of a tumor the surgeon will send the subject for a fMRI for pre-surgical mapping. Patients are typically required to perform certain tasks/paradigms. When the patient performs the tasks instructed, the blood flow in certain regions of the brain changes. This information is taken and used to develop images clearly showing the slice number and region of the brain being activated. These images are used by the neurosurgeon during brain surgery.



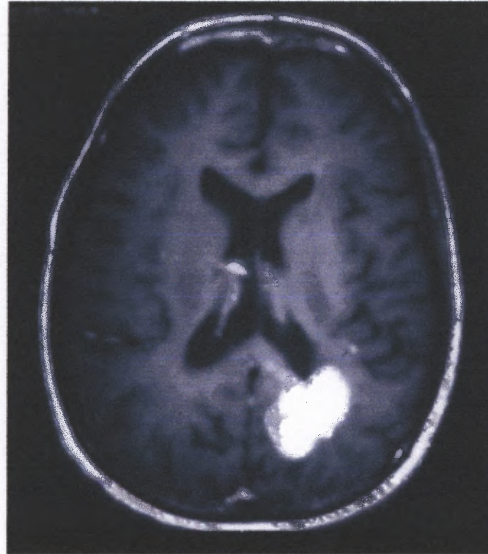


**Figure 3.2** MRI Image Showing Brain Tumor. The big white spot on the image is a tumor. [25]

Some commonly used tasks are bilateral finger tapping, text listening, silent word generation, and visual paradigms. These tasks are used to target different regions of the brain. Figure 3.3 clearly illustrates brain activation in the motor cortex. This image was obtained during a finger tapping paradigm. The activation is clearly shown in red.

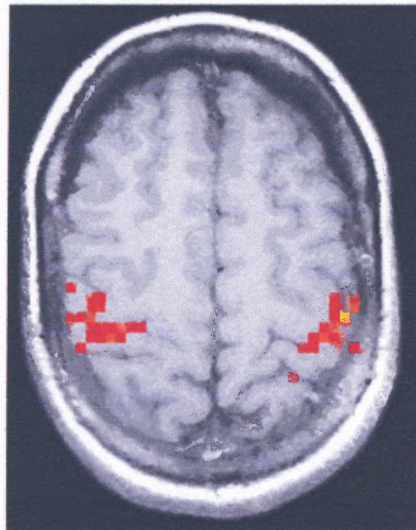


**Figure 3.3** fMRI Image Obtained During Finger Tapping Paradigm. Task was performed to activate the motor cortex. Image obtained from subject # 4 (slice # 18)

### **3.4 Using fMRI to Perform Surgery**

Functional MRI is a relatively new technology and research is being conducted to optimize this technology. Functional MRI is being used as a tool for brain mapping. Obtaining brain maps is a very useful tool for performing stereo-tactic brain surgery on patients with brain tumors. This technology can successfully indicate to the surgeon areas of the brain used when a patient is performing certain tasks/paradigm.

#### **3.4.1 Brain Mapping**

Brain mapping is used when the surgeon needs information from the brain which is activated when certain tasks are performed. There are several ways to map a patient's brain. Some are used during surgery; while others do not require craniotomy (opening the skull):

- Stimulating brain tissue with tiny electrical currents
- Measuring brain waves as they are stimulated
- Using ultrasound probes inside or near brain structures
- Probing the brain with special computerized wands
- Using special MRI techniques, such as PET (positron emission tomography), SPECT (single photon emission computed tomography), or fMRI.

PET is a test that assesses functional/metabolic activity in the tissue. The patient is given a radioactive substance (such as 18-FDG), by means of an IV injection, or in some cases, the patient will be asked to breathe in a gas with the substance (glucose,

carbon, nitrogen, oxygen, xenon which are altered to allow the emission of positrons). The compound travels through the blood to the area of the body under study. Depending on the drug administered it takes between 30 and 90 minutes for the substance to be absorbed by the tissue. The patient lies on a table and is moved into a machine that looks like a large, square-shaped doughnut. This machine detects and records the energy levels emitted from the substance that was injected earlier. The images are viewed on a nearby computer monitor.

As with PET when using SPECT the patient is given a radioactive substance through an IV injection in his/her arm. A few hours later, a scan is performed. During the scan, the patient will lie on his/her back on a special table, where he/she will need to remain very still. A gamma camera takes pictures over the next 30 minutes. From the pictures, the doctors can clearly see blood flow through the patient's brain.

fMRI is a noninvasive technique used to locate specific regions of the brain used when a subject performs certain tasks. The activated areas of the brain provide valuable information to the surgeon which help localize tissue that can be salvaged.

### **3.4.2 Stereo-tactic Surgery**

When the tumor is located, there are many treatment methods which can be used, to avoid damaging the surrounding tissue. When fMRI is performed, the patient is asked to perform certain repetitive tasks, or paradigms. Areas of the brain that control these functions will show increased activation on the scan, which can be transformed into an image showing the anatomical location of interest. This functional scan is then

overlapped with a conventional MRI image, in which an injection of a contrast medium (such as gadolinium) is used to show the outline of a tumor. [26]

Next, this combined scan is transferred to a surgical navigation computer in the operating room. Using this device, neurosurgeons routinely can guide incisions, skull openings, and brain tumor removal by the use of a special pointer whose position on a patient's head is matched to the corresponding point on an MRI or CT scan. With image-guided surgery, the location of the tumor can be noted, and removed with extreme accuracy. [26]

### **3.4.3 Possible Complications**

The complications common to all surgery apply to brain surgery such as bleeding, infection, and unexpected reactions to drugs and anesthetic agents. Because the brain is such a vital organ, neurosurgeons exercise phenomenal diligence in preventing complications. Whatever type of brain surgery is performed, complications unique to the brain may also occur:

- Convulsions also known as seizures occur whenever the brain is irritated. After surgery, the healing process, an infection, bleeding, residual tumor, or scar tissue may cause irritation. In many cases, it is necessary to take anti-convulsant medications. [18]
- Stroke is another complication that may be the result of brain surgery. It may be an inevitable result of the amount of brain tissue that had to be removed, or it can indicate damage to a blood vessel supplying a part of the brain. [18]

- Brain swelling may occur during or following brain surgery. It is important to watch for this very closely because it can lead to death. Prompt treatment to reduce the pressure from brain swelling is effective. [18]

The main problem associated with brain surgery to remove tumors is saving as much of the good tissue as possible. Currently, brain surgery is performed with anatomical images which are obtained from a MRI Scanner. A method to do the surgery with functional images in real-time has not been developed to date. Chapter 6 will describe a method of using functional images (showing activated voxels) in real-time while performing stereo-tactic brain surgery. This method will allow the neurosurgeon to see the activation points as he is performing the surgery. This will allow him to avoid cutting as much of the good tissue as possible.

## **CHAPTER 4**

### **DATA ANALYSIS METHODS**

#### **4.1 Introduction**

The statistical analysis of blood oxygenation level dependent data is a critical part of brain mapping with fMRI. Many statistical methods have been proposed, and there has been some debate about the most accurate approach. Given the flexibility of fMRI, and the range of experiments that is possible, it seems likely that a number of different statistical processing approaches can be applied to yield useful data. Applying several methods to the same data may be the best approach for evaluating fMRI data.

#### **4.2 Motion Correction**

Any motion during the acquisition of a magnetic resonance image can produce artifacts. Such motion includes subject movement, such as head motion, coughing, and swallowing. Physiological motions are also picked up during the scan, such as pulsatile blood flow, cerebrospinal (CSF) motions, and respiratory motions. In a conventional MR image, movement during a scan appears as a ghosting of diffuse blurring, which extends along the phase encoded direction over the full field of view of the image. [4]

The simplest interpretation of a dynamic series of MR images is that each image is measuring the net signal from an array of spatially defined voxels. The time course of a particular voxel is the average signal on a small volume of space centered at a position  $(x,y,z)$ . This position also corresponds to a fixed location in the brain. (AFNI, the post-processing software used to analyze functional images, clearly shows this axis with the

activated voxels when analyzing functional images). This is the theoretical explanation for why motion results in poor activation maps. Any slight movement of the subject's head will move parts of the subject's brain to different voxel locations. The typical signal change for activation is 5%, and for head motion is 15 – 25 %. If there are sharp edges in the intensity pattern of the image, such as near the edge of the brain, then movements much smaller than a voxel dimension can produce a signal change larger than the expected signal change due to BOLD effect. This causes a problem if the motion is correlated with the stimulus. (i.e. if the subject tips his/her head slightly when a visual stimulus is presented or if his head slides out of the coil slightly during a motor task, the result can be signal changes that correlate with the stimulus, but that are inaccurate.) A useful check is to be sure that activations are not right at a sharp boundary in the image. Often stimulus-correlated motion will present as a positive correlation on one side of the brain and a negative correlation on the other side of the brain, however this is not the only possible pattern. A good example of this is when superior axial slices are obtained at a level where the cross section of the factual activation around the edge of the brain is due to motion in the slice selection direction.

There are several approaches to dealing with motion artifacts. The best is to try and prevent motion as much as possible by carefully instructing the subject about the importance of remaining still, and by using head restraints. Foam pads between the coil and head, and the head and restraining strap are commonly used. Others have found that using a bite bar molded to fit the subject's teeth is a very effective method to limit head movement.

### 4.3 Separating true activation from noise

The most obvious processing strategy in identifying activated voxels would be to simply subtract the average of all the images made during the control task from the average of all the images made during the stimulus task. If the signal variations due to noise are in fact random having a normal distribution, and independent for each time point, this averaging will improve the SNR, thus it should provide a map of the activated areas. This naïve simplistic approach to data processing does not work well, and in practice data processing can become more involved. [4]

The first problem with the simple averaging scheme is that the standard deviation of the noise varies in different voxels so the noise is not uniform across the image plane. The noise infused into the signal from a particular voxel has two sources: random thermal noise and physiological fluctuations. The random thermal noise arises primarily from stray currents in the body that induce signals in the receiver coil. The thermal noise is spread throughout the raw acquired data, and when the image is reconstructed this noise is spread throughout the voxels of the image. The result is that this thermal noise can be accurately described as uniform random Gaussian noise, with the noise in the other voxels. If this thermal noise were the only source of fluctuations in the MR signal, the noise would have no spatial structure, but the variance of the signal over time measured in a human brain is several times larger than would be expected from thermal noise alone, and it exhibits both temporal and spatial structure. [4]

The additional variance of the MR signal in vivo is attributed to physiological fluctuations, which include several effects. Cardiac pulsations create a pressure wave that strongly affects the signal of flowing blood, but it also creates pulsations in the



cerebrospinal fluid (CSF) and in the brain parenchyma itself. Although these motions are small, they can easily produce signal fluctuations on the order of 1%, and the magnitude of the fluctuations varies strongly across the image plane. This is the central problem, created by non-uniform noise. When two noisy images are subtracted to calculate a difference image, if there is no activation in a voxel, the signals should subtract to yield a null image, but due to the nature of noise, there will be a residual difference, and the size of this random residual is on the order of the local noise standard deviation. Hence, the voxels with the largest signal fluctuations will show the largest random difference signal.

[4]

#### **4.4 The t-Test**

Among the statistical approaches used, one of the standard statistical parameters used to quantify the quality of a measured activation is the t-statistic. The t-statistic is closely related to the signal to noise of the difference measurement. In its simplest form, signals measured from a particular voxel are treated as samples of two populations (active and rest). The t-test is used to determine whether there is a significant difference between the means of the two groups. The t-statistic is a measure of how large the difference of the means is when compared to the variability of the populations. As t increases, the probability that such data could have arisen from two populations with equal means becomes more and more unlikely. This measure is quantified with the t-distribution, from which a researcher can calculate the probability that a particular value of t or larger could arise by chance if the means are identical. Then the process for analyzing BOLD data begins with the calculation of the t-statistic for each voxel. A threshold value of

probability, such that  $p < .01$ , which corresponds to a particular threshold on  $t$  is selected. All voxels whose  $t$ -value pass the threshold are selected. These voxels are then displayed as activated in color on an underlying map of the anatomy for each case of visualization. [4]

The choice of a threshold on  $t$  for constructing the activation map involves consideration of the fact that the signals from many voxels are being measured simultaneously. (i.e. if the researcher was considering the difference of means of only a single voxel, he/she could adopt the conventional criterion that  $p < .05$ . The measured difference is considered to be significantly different from zero.) When accessing a whole brain fMRI study, there could be approximately 10,000 brain voxels that are analyzed, and at this level of significance only about 500 voxels appear to be active. To account for these multiple measurements, a more conservative  $p$  value has to be used. To reduce the probability of finding any false positive activations to the 5% level, the  $p$ -value should be 5% divided by the number of voxels. This is known as Bonferroni correction. [4]

#### 4.5 Correlation Analysis

The statistical analysis can be enlarged to include the expected hemodynamic response with a correlation analysis. Instead of assuming that the hemodynamic response precisely matches the stimulus pattern, delay and smoothing are incorporated by defining a model response function. A simple approximation for the model response to a block stimulus pattern is a trapezoid. This trapezoid has 6-s ramps delayed by 2-s from the onset of the stimulus block. Having chosen a model response function, each measured voxel time course is analyzed by calculating the correlation coefficient  $r$  between the data

and the model function. The correlation coefficient ranges from -1 to 1 and expresses the degree to which the measured signal follows the model function. The correlation coefficient is then used as the statistical parameter for mapping, and a threshold on  $r$  is chosen to select pixels that are reliably activated. Figure 4.1 shows an example of an activation map calculated from the correlation coefficient map. This image was obtained from subject # 4 (slice # 9) during a text listening paradigm. The respective BOLD signal is shown in figure 4.2.

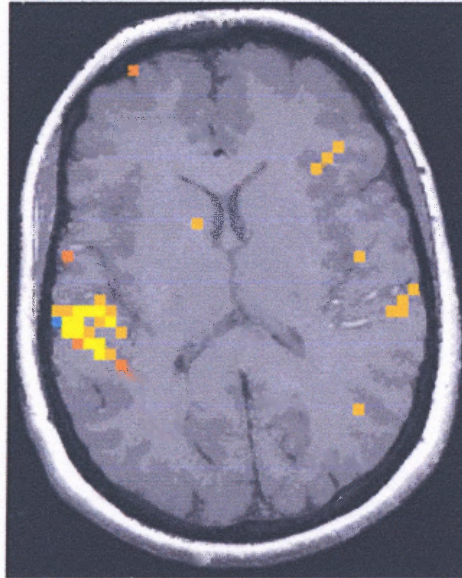


**Figure 4.1** FMRI Image Obtained Using Cross-Correlation. Image clearly illustrates activated voxels in the Wernicke's area of brain.



**Figure 4.2** BOLD Signal Obtained from Text Listening Paradigm.

Correlation Analysis is similar to the simple t-test comparison of means (discussed in section 4. 5). Correlation analysis is a more general approach, because it allows one to use any model function, so the true response can be better approximated. Correlation analysis is a component of a more general linear regression analysis. In correlation, researchers try and model the data as a linear combination of one or more model functions plus noise.

#### 4.6 Fourier Imaging

Another method of analyzing BOLD data for block design is to calculate the Fourier Transform of the measured time course, and examine the component at the fundamental

frequency of the stimulus pattern. If four cycles of stimulus are performed, the magnitude of the four cycle frequency in the Fourier spectrum should clearly show a spike whenever activation is present. Figure 4.3 depicts a blocked stimulus pattern, the hemodynamic response, and the stimulated data with the addition of noise. The stimulus pattern shows a prominent fundamental frequency, and a series of odd multiples of the fundamental frequency. [4]

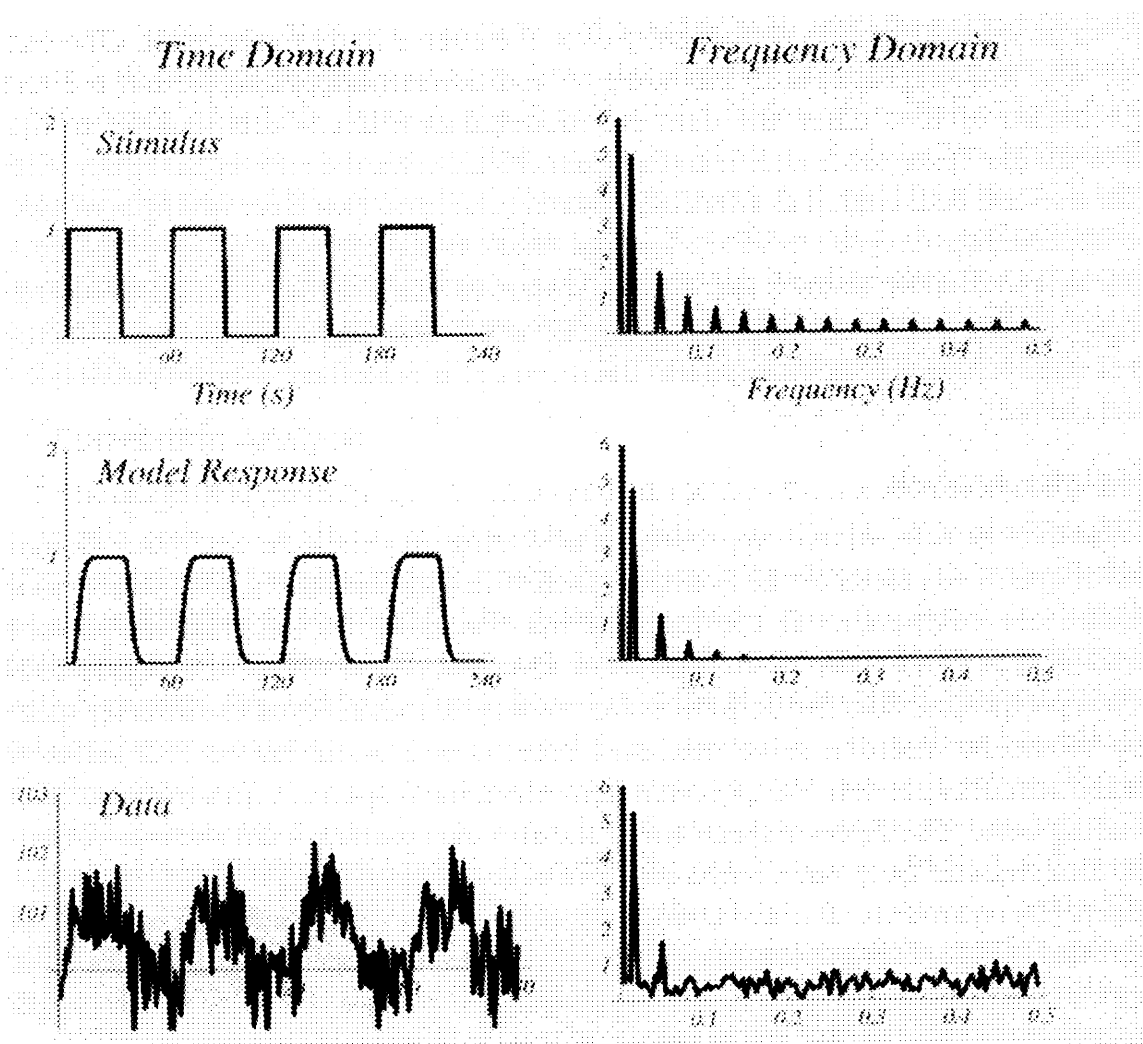


**Figure 4.3** Fourier Components of the BOLD Signal. Stimulus shown are top, Model response in the middle, and Data at the bottom. [4]

A Fourier analysis has additional advantages, for a select few applications where the delay of the response can be calculated with little difficulty. There is much evidence that hemodynamic delay may vary from one region of the brain to the other. This presents a problem with the standard correlation analysis. If the delay used in the model for the hemodynamic response function does not match the true delay, then the correlation coefficient would be reduced, and the activated pixels could be missed. To account for this dilemma, the correlation coefficient for the same model shape with different delays can be calculated. The correlation coefficient giving the highest value of  $r$  is chosen as the best fit for that voxel data. [4]

Another way of looking at a Fourier transform analysis in the context of correlation analysis is to see that the comparison of a data time course with a model response function can be accomplished in the time as well as frequency domain. The Fourier transform of the model response function depicts spikes at multiples of the fundamental stimulus frequency, and the relative amplitudes and phases of these spikes depend on the shape of the response function in the time domain. This is clearly illustrated in figure 4.3. The Fourier transform of an activated pixel will also show spikes at the same frequencies. The correlation analysis hence is equivalent to comparing the amplitudes of the model and data frequency spectra. The data are compared at the fundamental frequency and each harmonic. Then a determination is made whether these amplitudes in the data are sufficiently larger than the noise. [4]

#### 4.7 The Kolmogorov-Smirnov Test

Another statistical test used to evaluate the statistical significance of detected activations in a block design experiment is known as the Kolmogorov-Smirnov Test (KS test). Similar to the t-test, the KS test treats the signal values measured during the task and control periods as two populations, and then tests whether the two populations vary significantly. The KS test is a non-parametric test, unlike the t-test which is a parametric test. With the t-test, the main goal is whether the cumulative distributions of the two populations are significantly different. For each population, the measured values are organized in ascending order. A very good estimate of the cumulative distribution is determined by calculating  $P(x)$ , the fraction of signal values greater than  $x$  for each  $x$ . From the two distributions  $P_{act}(x)$  and  $P_{rest}(x)$ , the KS statistic is calculated as the maximum difference between the two cumulative distributions. Using the null hypothesis, the distribution of the KS static can be calculated, so the significance of any measured value can be determined. [4]

In general, the KS test is less sensitive than the other approaches described in this chapter. Some weak activations could be missed with the KS test, but the ones that are deemed to be significant are likely to be highly reliable. One interesting aspect of the KS test is that in principle it could detect a difference between the two populations which have the same mean but different standard deviations. If the variance of the MR signal changed with activation, the KS test could potentially detect this change. Such a physiological effect has not been observed, so whether this mathematical property has any significance for brain activation studies is not known. [4]

#### 4.8 Noise Correlations

The complete determination of the importance of detected activation points depends on a comprehensive understanding of the noise in the data, as well as noise in the BOLD measurements of the brain. This is still not understood in a quantitative way. When referring back to the simplest method of a t-test, (comparison of the mean signals) to determine the significance of the measurement of a particular value of  $t$ , the degrees of freedom are required, which are essentially the number of independent measurements used in the calculation. (i.e. Only two measurements are taken, each in the stimulus and control states. A value of  $t > 3.0$  or larger is borderline significant ( $p = .029$ ), but with 50 measurements in each state,  $t > 3.0$  is highly significant ( $p = .0017$ .) These estimates of the significance of  $t$  are based on two assumptions regarding noise. First, the noise is normally distributed, and second the noise in each measurement is independent of the noise in the other measurements. [4]

Structured noise will always remain a problem for the analysis of BOLD data, and further work is required to understand these signal fluctuations better, so they can be taken into account in the statistical analysis.

#### 4.9 Reliability of Activation

An important issue in the interpretation of the BOLD studies is the accuracy of the localization. Because the venous vessels undergo the largest changes in deoxyhemoglobin content, the largest BOLD changes are likely to occur around draining veins. Such veins may be removed from the area of neuronal activation, so the location



of the BOLD change could differ by as much as a centimeter or more from the area of increased neuronal activity. [4]

The reliability of activation varies from subject to subject. Motion is one of the key factors in obtaining reliable activation maps. If a subject can remain still for the entire length of the scan and perform the tasks properly, reliability will be substantially improved. The image obtained from a subject like this will be very accurate, and may not require extensive post-processing. Unfortunately this is not feasible, and a subject can never fall into this scenario, because motion and physiologic artifacts are unavoidable.

There are ways to correct motion and remove noise. The methods discussed earlier are currently being used to remove noise in these MR images. Correlation, t-test, and Fourier are among the few imaging methods currently used to obtain reliable activation maps. The new method discussed in chapter 5 is another analysis tool that researchers can use to obtain more reliable images. In this method the amount of time points and thresholds were varied to determine the optimal number of time points to obtain the most accurate image. Functional MRI is a fairly new method of obtaining images, and the reliability will improve as more techniques and more advanced equipment is developed. If a real time system is developed to show activation maps as the subjects are being scanned, the reliability will be improved significantly. Instead of waiting to reconstruct the data, this will give researchers information they need in real-time. If the scan yields unreliable data, it can be repeated until the image acquired is satisfactory. There are many image processing techniques available but new methods will always be developed to improve the reliability of the images obtained.

## **CHAPTER 5**

### **THE EXPERIMENT**

#### **5.1 Introduction**

Eight healthy human subjects (four men and four women with no history of head trauma or neurological deficit) between the ages of 18 – 60 years were scanned after obtaining a written consent. All protocols in this study were approved by Institutional Review Board (IRB). The  $dB/dt$  (change in the magnetic field because it causes a current) limit in all experiments was kept below that specified by the FDA. All subjects were paid on an hourly basis. Subjects were placed in the supine position with their head adjusted for symmetry along the midline. Foam padding between the head and coil was used to reduce motion.

All images were obtained on a 3T Siemens Allegra (Ehrlagen, Germany) imaging system. The imaging system was equipped with a three axis balanced torque head gradient coil and a shielded end cap quadrature transmit/receive birdcage radio-frequency coil. Thirty axial slices (of echo-planar images) spanning the entire brain were scanned. Imaging parameters used are as follows: FOV=20x20 cm<sup>2</sup>, slice thickness = 5 mm, Matrix = 64x64, TR =2 sec, TE = 27 msec. Ninety sequential images were obtained during each run. Each subject was instructed to perform three tasks.

During the first scan, subjects performed bilateral finger tapping to activate the sensory motor cortex (figure 5.1, 5.2). The scan consisted of 20 seconds of rest alternating with 20 seconds of bilateral finger tapping. For the second and third scan, silent word generation and text listening paradigms were presented to activate the

Wernicke's area of the brain (figure 5.3). Similarly these tasks consisted of 20 seconds of rest alternating with 20 seconds of activation. The length of each scan was 180 seconds enabling the entire stimulus to proceed.

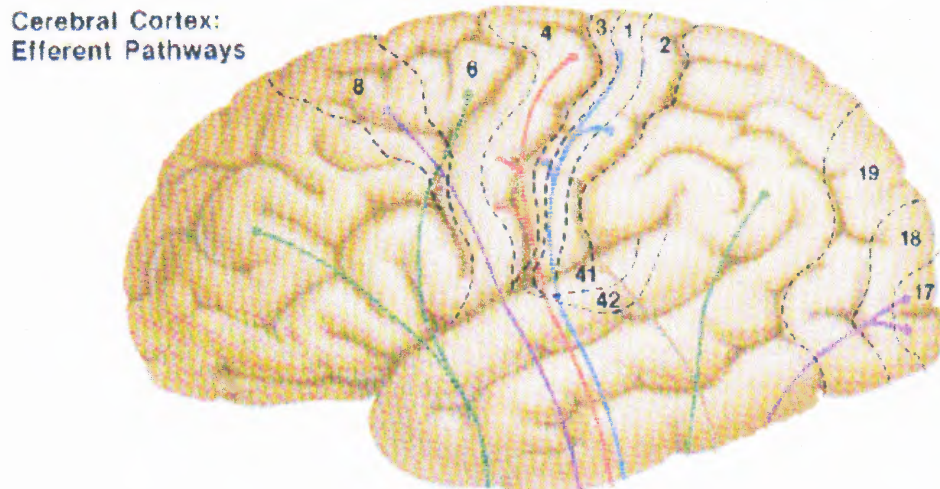


**Figure 5.1** Sagittal View of Motor Cortex. Area 4 is activated when bilateral finger-tapping is instructed. [15]

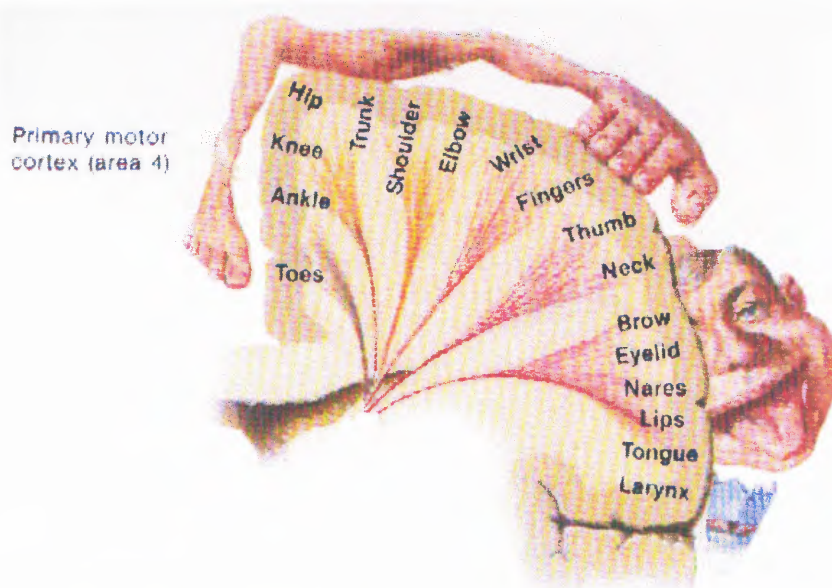


**Figure 5.2** Axial View of Motor Cortex. Shows area activated when bilateral finger-tapping is performed. [15]

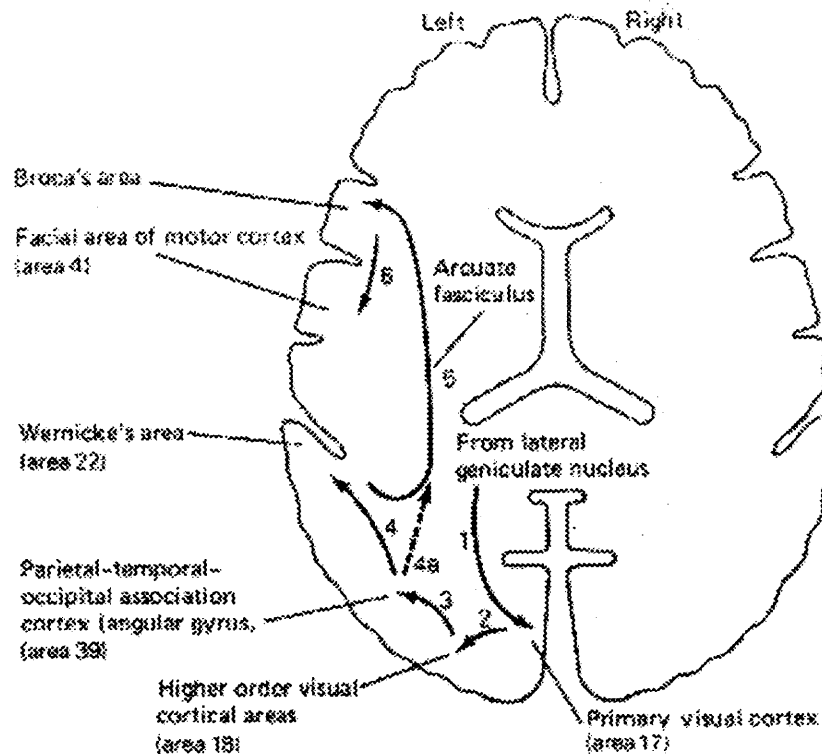


**Figure 5.3** Axial view of Wernicke's Area. [27]

## 5.2 Steps Taken to Scan a Subject and Analyze the Data

The steps taken to scan a subject and analyze the data are as follows:

- I. Each subject was given instructions about the tasks he/she would be asked to perform while in the MRI scanner. Each subject was warned about the noise that he/she would experience when inside the machine, and was told not to be frightened. The following tasks were explained to each subject before the scanning began.

- **Bilateral Finger Tapping** – Each subject was instructed on how to perform bilateral finger tapping. The subject was instructed to tap his/her fingers on both hands as rapidly as he/she could when he/she heard the signal “tap”, and was instructed to stop when he/she heard “stop”. In addition to giving a verbal description of the task, each subject was also given a physical demonstration on how to perform finger tapping.
- **Silent Word Generation** – The second task instructed to each subject was silent word generation. In silent word generation each subject was given a letter. When the subject heard the letter he/she was instructed to think of as many words beginning with that letter silently in his/her head until he/she was instructed to “stop”. In addition to this if for some reason the subject was unable to hear the letter; he/she was instructed to make up his/her own letter and think of as many words beginning with the new letter as possible. The results will not be altered if the subject thinks of his/her own letter, because the same region of the brain (Wernicke’s Area) will be activated. The letters used were kept constant in all subjects (R, S, T, L were used). Subject # 8 performed this task twice, and for the second scan the following letters were used: G, B, D, H
- **Text Listening** – The final task instructed to each subject was text listening. In text listening, the subject was instructed to concentrate on the text when it was read to him/her. The subject was asked to comprehend as many words as he/she could in spite of all the noise in the scanner room. Even if a few words were understood activation maps could be obtained.

The stimulus paradigm used for this study is shown in figure 5.4. It is very important to choose a stimulus paradigm that will allow enough time to show significant hemodynamic response. This project called for a TR = 2 with 4 cycles of 20 seconds of activation followed by 20 seconds of rest. The same stimulus paradigm was used for all tasks that the subjects were instructed to perform.

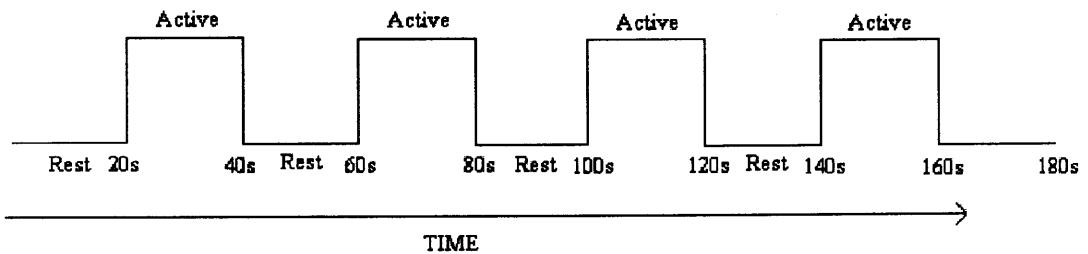


**Figure 5.4** Stimulus Paradigm.

II. As the scanning progressed the data were saved to the Siemens computer (running Windows). After the scanning was completed, the data were transferred to a different computer where the functional images could be analyzed in AFNI. Before the images could be analyzed in AFNI, the raw data acquired from the 3T Siemens MRI Scanner had to be reconstructed. The program used to alter the file images (written by Dr. Bharat Biswal) is shown in the Appendix B. After the data were reconstructed, the “to3d” command was used to change the file format from dicom (acquired from MRI scanner) into .brik and .head files (what AFNI can read). To3d reads in a collection of 2D images and formats them into an AFNI dataset.

- III. Finally, after the data was reconstructed the images were analyzed using a popular public domain software called AFNI. Activation maps were created, the number of time points were varied, and functional images were altered in the most effective way to obtain the most favorable image.

### 5.3 Motion Corrected Data

Subject motion during the time course of functional activation studies has been shown to cause spurious signals which can mimic true activation. Therefore, the importance of motion correction has been widely recognized. Correction with post-processing using image registration software is a common practice in functional imaging and analysis. Many image registration algorithms, developed for analysis requirements other than fMRI, assume rigid body motion. Although these techniques are now routinely used by a number of groups, rigid body co-registration has not yet been shown to reduce the effects of motion to an acceptable level in fMRI analysis. [4]

After data collection, motion effects can be corrected with post processing software. AFNI was used to perform motion correction for the data obtained in this study. The primary goal of such techniques is realignment of MR images. If the motion takes place in the plane of images, then a two-dimensional registration is adequate. (i.e. If the subjects head tipped forward, with no rotational component, and the images are sagittal in orientation, then motion is entirely in one plane of the image. The correction is then a translation and rotation to optimally align the image with a reference image.) The corrections required to motion correct an image are subpixel shifts, so the new image matrix is an appropriate interpolation of the original image onto the new registered grid.

If the motion does not exist on the image plane, then a three dimensional registration is required. In addition to being a more time consuming calculation, the problem with 3D registration is that 2D images are acquired sequentially in time. This means that at any one time point a complete 3D image is not available to compare with a 3D image at another point in time. This is a problem, however schemes have been developed to address this problem. [4]

Tables 5.1 through 5.8 show the calculated motion for each subject for each task performed. The mean and standard deviations were calculated, using the program Matlab. The script file used to calculate these values is shown in Appendix A. The abbreviations used in the following tables are as follows:

A – P = Head Motion from Anterior to Posterior

R – L = Head Motion from Right to Left

I – S = Head Motion from Inferior to Superior

STD = Standard Deviation

**Table 5.1** Motion Corrected Data for Subject #1  
Scanned August 10, 2004

Task	Finger Tapping		Silent Word Generation		Text Listening	
	Mean	STD	Mean	STD	Mean	STD
Yaw	-0.2335	0.0893	-0.0273	0.0333	0.0620	0.0354
Pitch	-0.1705	0.1044	-0.2388	0.1287	0.0141	0.0413
Roll	-0.0862	0.0643	-0.0212	0.0508	0.1732	0.1349
A – P	-0.0607	0.2064	-0.2306	0.1811	0.4162	0.3144
R – L	-0.6575	0.2530	-0.1030	0.0575	0.0402	0.0343
I – S	-0.0411	0.0429	-0.0404	0.0575	0.0284	0.0694



**Table 5.2** Motion Corrected Data for Subject # 2  
Scanned September 15, 2004

Task	Finger Tapping		Silent Word Generation		Text Listening	
	Mean	STD	Mean	STD	Mean	STD
Yaw	-0.0310	0.0308	-0.0701	0.0432	0.1591	0.0913
Pitch	-0.4609	0.2129	-0.0061	0.1145	-0.5099	0.2752
Roll	0.0205	0.0490	0.0219	0.0131	0.0677	0.0397
A – P	0.7531	0.3597	-0.0484	0.0385	0.1724	0.0763
R – L	-0.0614	0.0308	-0.0784	0.0399	0.2032	0.0905
I – S	0.0620	0.0265	-0.0056	0.0535	-0.2103	0.0934

**Table 5.3** Motion Corrected Data for Subject # 3  
Scanned October 18, 2004

Task	Finger Tapping		Silent Word Generation		Text Listening	
	Mean	STD	Mean	STD	Mean	STD
Yaw	0.2349	0.0958	-0.0195	0.0364	-0.0693	0.0475
Pitch	-0.0660	0.1624	0.6002	0.3148	-0.0336	0.0814
Roll	0.0378	0.0448	-0.0791	0.0640	-0.0409	0.0240
A – P	0.2997	0.1945	-0.3759	0.3333	0.2242	0.1654
R – L	0.1699	0.0688	-0.0904	0.0573	0.0820	0.0477
I – S	-0.6058	0.3283	-0.1385	0.1171	-0.0875	0.0526

**Table 5.4** Motion Corrected Data for Subject # 4  
Scanned October 21, 2004

Task	Finger Tapping		Silent Word Generation		Text Listening	
	Mean	STD	Mean	STD	Mean	STD
Yaw	-0.0569	0.0338	0.0476	0.0436	-0.0271	0.0627
Pitch	0.1888	0.1101	0.3773	0.2191	0.0633	0.0419
Roll	0.0414	0.0336	0.0744	0.0327	0.0172	0.0290
A – P	0.-692	0.0433	-0.1158	0.0514	0.0268	0.0273
R – L	0.0229	0.0316	0.0623	0.0380	-0.0276	0.0584
I – S	0.0304	0.0295	-0.1139	0.0720	-0.0103	0.0241

**Table 5.5** Motion Corrected Data for Subject # 5  
Scanned October 25, 2004

Task	Finger Tapping		Silent Word Generation		Text Listening	
	Mean	STD	Mean	STD	Mean	STD
Yaw	0.0088	0.0340	-0.0051	0.0180	-0.0720	0.0472
Pitch	-0.0644	0.0231	0.1343	0.0907	-0.0621	0.1390
Roll	0.0013	0.0167	0.0389	0.0350	0.0595	0.0568
A – P	0.0954	0.0422	-0.0889	0.0607	0.0244	0.0490
R – L	0.0251	0.0256	-0.0105	0.0182	0.0388	0.0551
I – S	0.0025	0.0168	-0.0975	0.0624	-0.0629	0.2293

**Table 5.6** Motion Corrected Data for Subject # 6  
Scanned October 27, 2004

Task	Finger Tapping		Silent Word Generation		Text Listening	
	Mean	STD	Mean	STD	Mean	STD
Yaw	0.0763	0.0883	0.8837	0.4118	1.1951	0.7496
Pitch	-0.6233	0.3020	0.0270	0.2847	-0.3738	0.7402
Roll	0.1361	0.1464	0.7143	0.3255	0.4724	0.3026
A – P	0.6401	0.3260	0.5959	0.6215	0.2734	0.6260
R – L	0.2043	0.1424	1.0001	0.4563	1.8912	1.0706
I – S	-0.1790	0.1131	-0.1684	0.1857	-0.0482	0.1128

**Table 5.7** Motion Corrected Data for Subject # 7  
Scanned October 27, 2004

Task	Finger Tapping		Silent Word Generation		Text Listening	
	Mean	STD	Mean	STD	Mean	STD
Yaw	0.2669	0.1430	0.0393	0.0652	0.5087	0.3654
Pitch	-0.0756	0.1566	-0.1257	0.0911	-0.3312	0.1714
Roll	-0.0340	0.0448	-0.1437	0.1106	0.1749	0.1207
A – P	0.0441	0.0957	0.2096	0.1656	0.0194	0.0759
R – L	0.2099	0.1417	-0.0306	0.1516	0.7546	0.4741
I – S	0.0991	0.1145	-0.0114	0.0453	0.0799	0.0585

**Table 5.8a** Motion Corrected Data for Subject # 8 (Session 1)  
Scanned October 29, 2004

Task	Finger Tapping		Silent Word Generation		Text Listening	
	Mean	STD	Mean	STD	Mean	STD
Yaw	0.1656	0.1240	0.0365	0.0441	-0.0108	0.0253
Pitch	0.0551	0.0274	0.0808	0.0542	-0.1022	0.0534
Roll	0.2467	0.1561	0.0331	0.0228	0.0293	0.0248
A – P	0.0664	0.0421	-0.0489	0.0470	0.0187	0.0403
R – L	0.2559	0.1938	0.0822	0.0889	-0.0199	0.0320
I – S	-0.1533	0.1005	-0.1109	0.0774	-0.0666	0.0531

**Table 5.8b** Motion Corrected Data for Subject # 8 (Session 2)

Task	Finger Tapping		Silent Word Generation		Text Listening	
	Mean	STD	Mean	STD	Mean	STD
Yaw	0.1378	0.1033	0.0422	0.0228	0.0339	0.0240
Pitch	-0.2150	0.1450	0.0656	0.0694	0.0424	0.0158
Roll	0.6510	0.3363	-0.0041	0.0147	0.0555	0.0319
A – P	0.0757	0.0702	-0.0733	0.0515	0.0487	0.0429
R – L	0.4486	0.2849	0.1031	0.0514	0.00004	0.0201
I – S	-0.1742	0.1081	-0.0869	0.0574	-0.0649	0.0499

Motion correction is an essential step in obtaining an image that can be used during stereo-tactic surgery. Figure 5.5a and 5.5b clearly show an image before and after motion correction respectively.

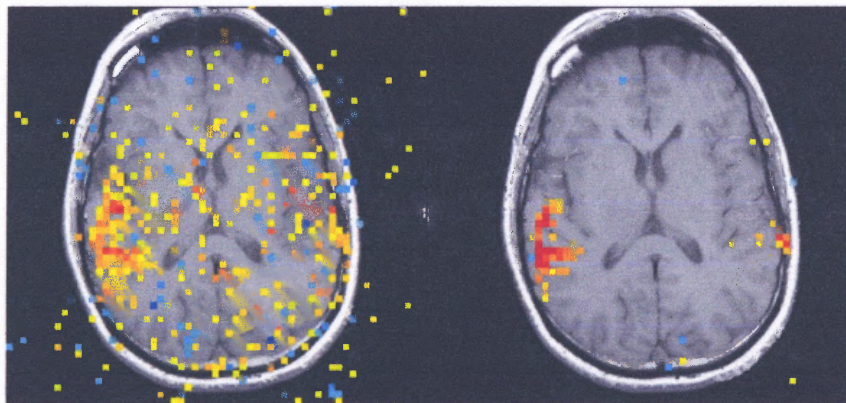


**Figure 5.5** (a-left) FMRI Image Obtained from a Text Listening Paradigm Before Motion Correction. Image shown is slice # 8 from subject # 3. (b-right) FMRI Image after Motion Correction.

There are a few other problems due to motion that need to be corrected in addition to image registration. The first is the spin history effect. With a reasonably short TR, the MR signal is not fully relaxed, but if everything is repeated exactly the same, a steady state develops such that with each repetition, the signal generated is the same. If motion causes a group of spins to move out of a selected slice, then these spins will not be influenced by the next RF pulse. If they are later moved back into the slice, their spin history will be different from that of spins that remained within the selected slice. This disrupts the steady-state signal in a way that depends on the past motion. This effect can be estimated by using the history of the motion estimated from the image registration algorithm. [4]

A more subtle motion correction problem is if basic picture is not correct. MRI measures the signal from a set of fixed voxels in space. Magnetic field variations within the head distort the image obtained. This results in problems with aligning EPI images with higher resolution (anatomical images that are less sensitive to motion). Because the source of the distortions is the head, any motion will shift the pattern of distortions. Basically the location in space corresponding to a particular voxel is not fixed. This fact adds another layer of complexity to motion correction that researchers are beginning to address. [4]

#### **5.4 Determining Optimal Data Length for fMRI Images**

The magnetic resonance signal change during activation due to BOLD effect is quite small, on the order of 1% for a 50% change in cerebral blood flow (CBF). To use these weak signals for brain mapping, they must be reliably separated from the noise. With

echo planar imaging (EPI), the intrinsic signal-to-noise ratio (SNR) in a single-shot image is often quite large, in the range of 100-200, but this is still not large enough to reliably detect a 1% signal change in a voxel from a single image in the stimulus state and a single image in the control state. For this reason, an optimal number of images are required to allow sufficient averaging to detect small signal changes.

Cross-correlation was used to detect and identify the activated voxels. To study the effect of data length on the correlation analysis, both the number of voxels which passed the threshold, as well as the mean correlation coefficient were analyzed. During each run, the number of time points varied from 40 to 90 with increments of 5. The threshold (cross-correlation threshold) was also varied from .35 to .60 with increments of .05. The number of activated voxels, and the mean correlation coefficient were calculated for each time-point and threshold.

Figures 5.6 and 5.8 were obtained from subject # 3 during a text listening, and finger tapping paradigm, respectively. These figures illustrate how varying the number of time points alters the reliability of activation. These functional MR images were obtained by varying the number of time points from 15 to 90. This gives an excellent idea of the results obtained from this study.

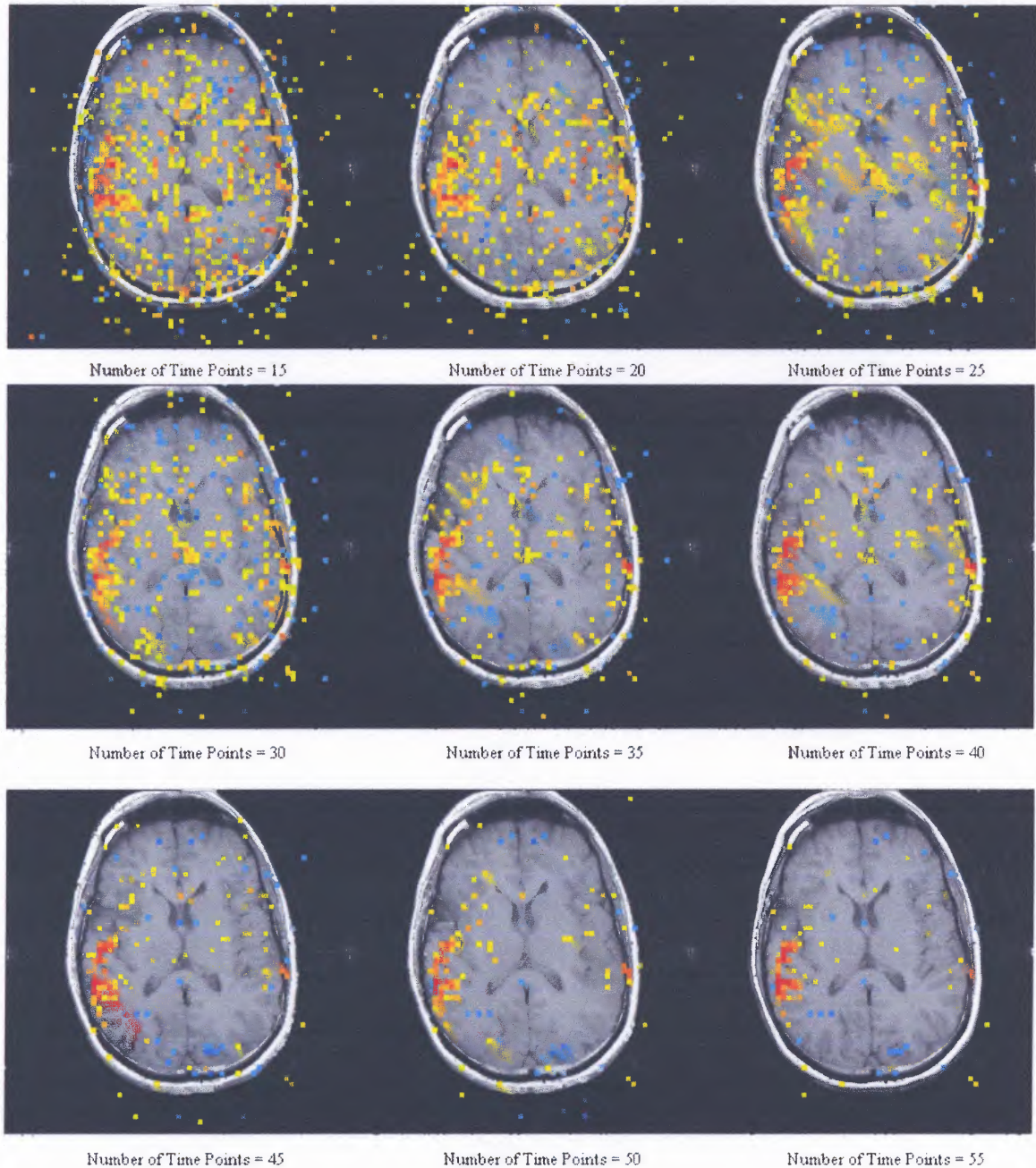


**Figure 5.6a** Images Obtained by Varying Number of Time Points from 15 – 55 during a Text Listening Paradigm. FMRI images obtained from subject # 3 (slice # 9).

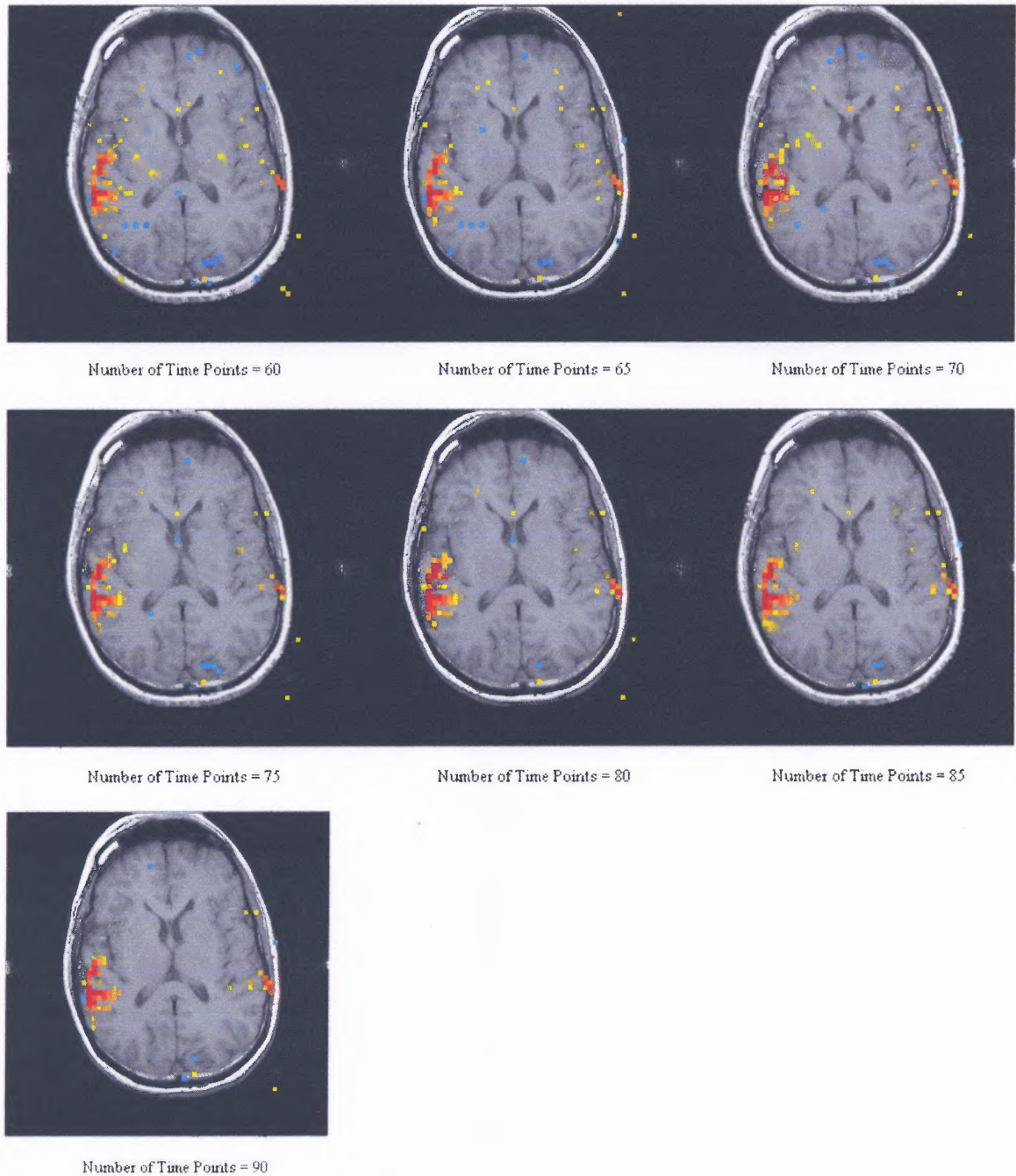


**Figure 5.6b** Images Obtained by Varying Number of Time Points from 60 – 90 during a Text Listening Paradigm. FMRI images obtained from subject # 3 (slice # 9). This is a continuation of figure 5.6a.

Figure 5.6a and b clearly illustrate how varying number of time points and using cross-correlation significantly improved the usage of an image. A graphical

representation showing the number of activated voxels as the number of time points were varied is shown in figure 5.7c for the text listening paradigm. If one were to use the image obtained with 15 time points all that can be seen is noise. It cannot be used during surgery, because it does not give an accurate location of the activation points. As the number of time points was increased, the noise slowly started to disappear. Sometimes using too many time points was also detrimental, and did not yield the most accurate results. The number of time points plateaued around 60. This can be seen in figure 5.7. Figures 5.7b and d show graphs obtained from subject # 3 during the silent word generation and finger tapping paradigms, respectively. Figure 5.8a and b show another example of how varying the number of time points altered the image by reducing noise. The images in figure 5.8 were obtained from the same subject (slice # 18) during a finger tapping paradigm. The data from these images can be seen in figure 5.7d in a graphical representation. The graphs shows how the number of activated voxels varied as the number of time points and thresholds were varied. Figure 5.7a is the legend used for the graphs shown in figure 5.7 b, c, and d.

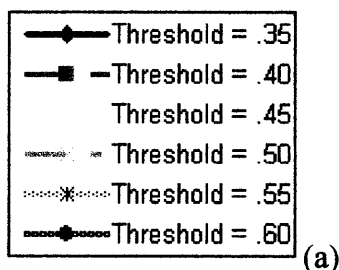


**Figure 5.7** (a) Legend Used for Figures 5.7b, c, and d. (b) Number of Activated Voxels from Silent Word Generation Paradigm, (c) Number of Activated Voxels from Text Listening Paradigm, (d) Number of Activated Voxels from Finger tapping Paradigm.



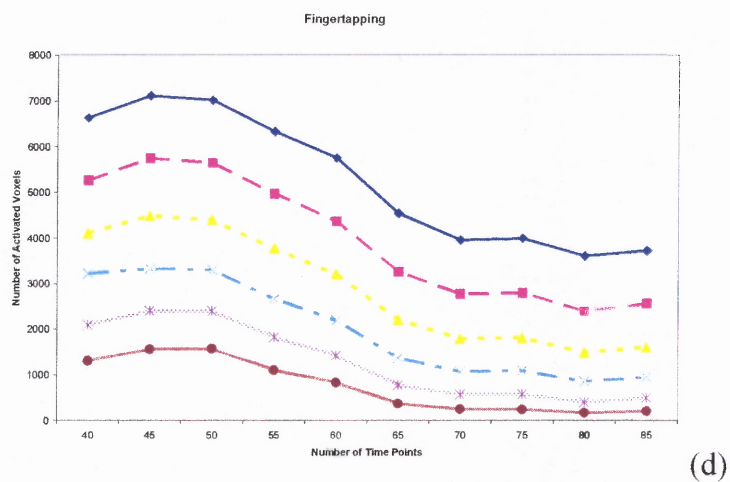
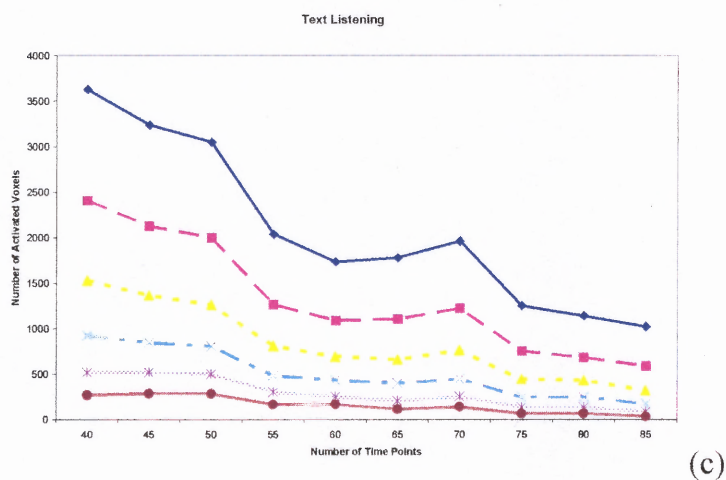
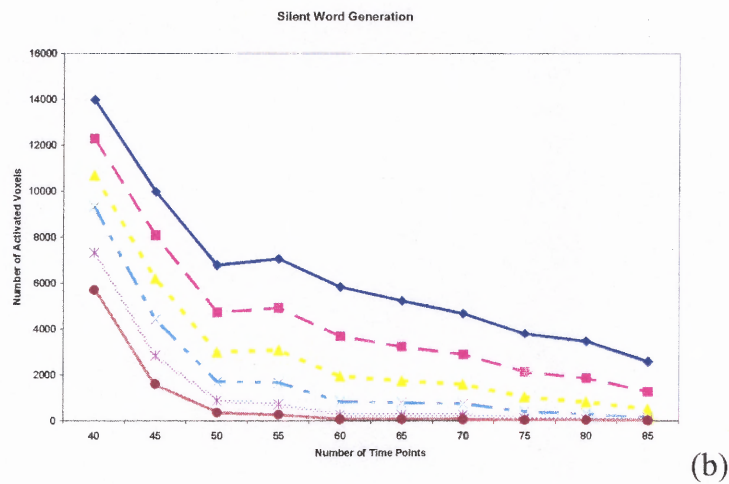
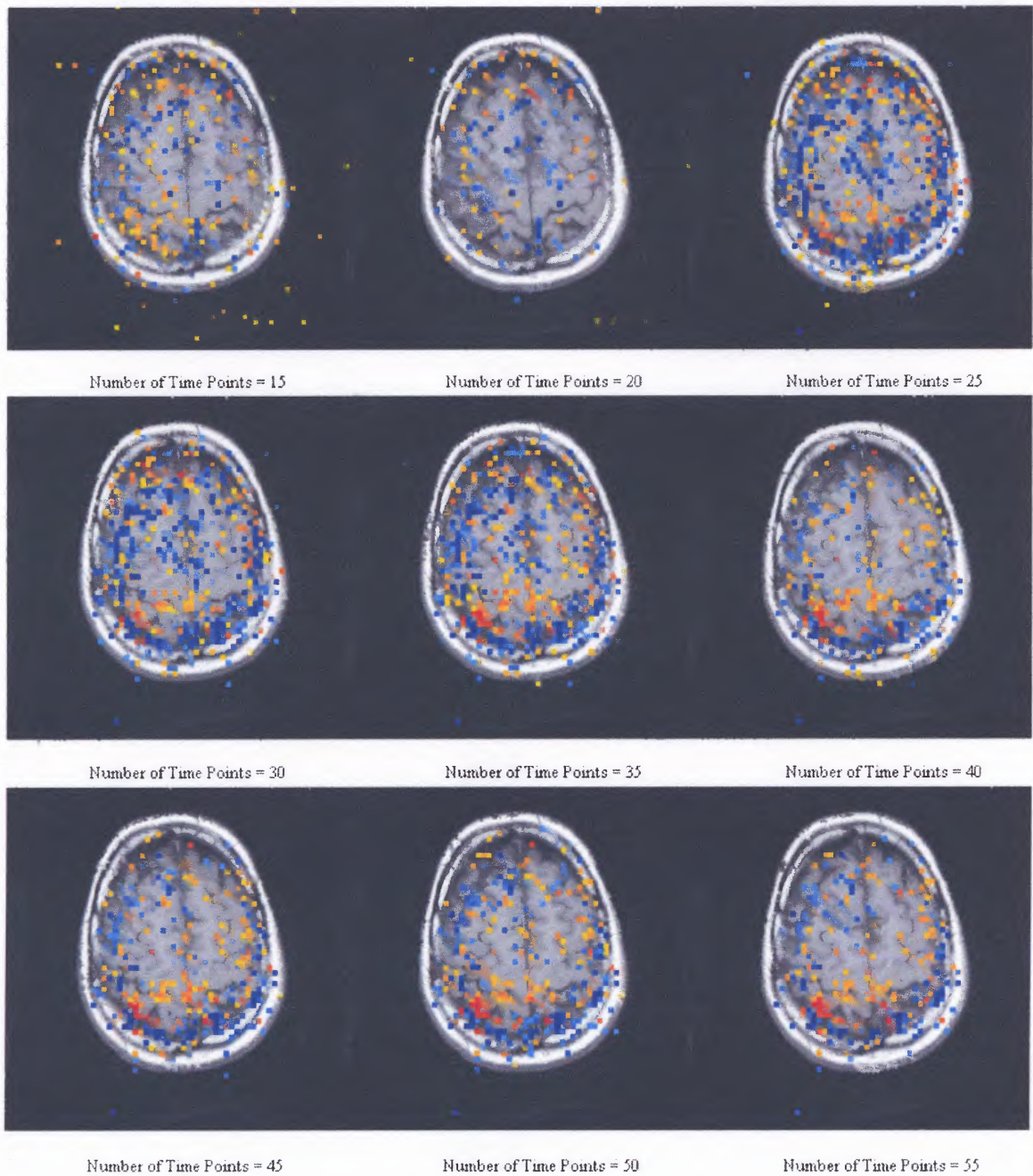
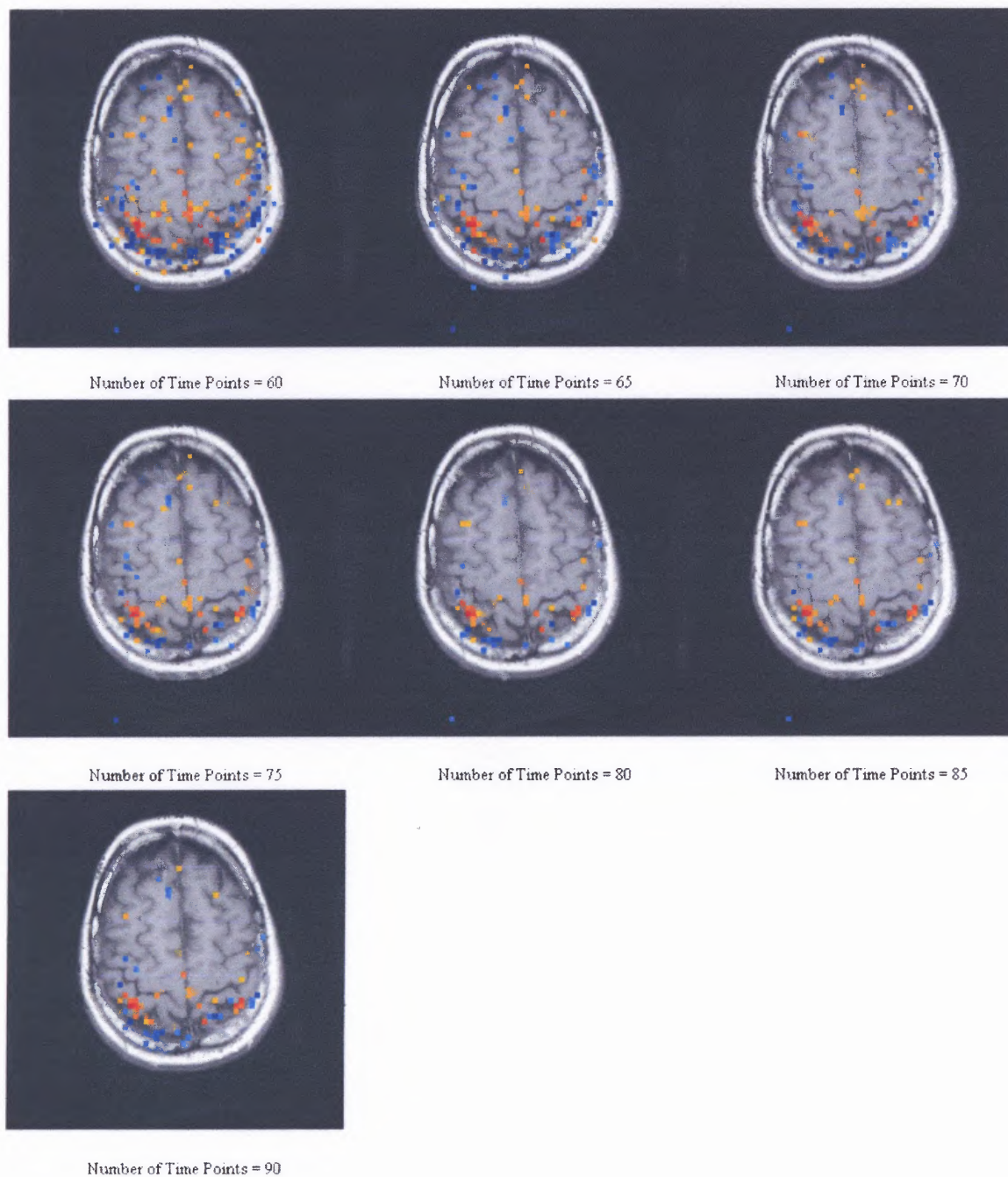


Figure 5.7 (Continued)



**Figure 5.8a** Images Obtained by Varying Number of Time Points from 15 – 55 during a Finger Tapping Paradigm. FMRI images obtained from subject # 3 (slice # 18).



**Figure 5.8b** Images Obtained by Varying Number of Time Points from 60 – 90 during a Finger Tapping Paradigm. FMRI images obtained from subject # 3 (slice # 18). This is a continuation of figure 5.8a.

## 5.5 Results

The number of activated voxels during typical silent word generation, text listening, and finger tapping paradigm from a representative subject is displayed for various data lengths and thresholds (Figure 5.7). Figure 5.7 clearly shows that after approximately 60 time points, the number of activated voxels plateaus. Similarly, the optimal number of time points for each scan from each subject is shown in Table 5.9. As can be seen from Table 5.9 in most of the cases, the activated response is stabilized by 60 time points. This result would imply that for various fMRI studies, 60 time points can be used to reliably detect activation induced signal changes in the brain. A block paradigm was used to generate the stimulus. For more complex tasks such as event-related designs, a similar analysis can be performed to determine the minimum number of time points required to achieve stability.

**Table 5.9** Optimal Number of Time Points for each Subject Scanned

Task	Subject #							
	1	2	3	4	5	6	7	8
	Optimal Number of Time Points							
Finger Tapping	60	60	70	65	60	60	60	70
Silent Word Generation	60	65	65	65	60	65	60	60
Text Listening	65	65	60	60	65	65	60	60

## CHAPTER 6

### DEVELOPMENT OF FILE CONVERSION SOFTWARE

This part of the project was performed to convert functional magnetic resonance images from Tiff format to Dicom format. The neurosurgeon's scanner was unable to read the functional magnetic resonance images being developed from AFNI. The surgeon wanted to use these images during stereo-tactic brain surgery in real-time. This was not feasible until this program was developed. The program used to accomplish this task was created using Matlab. The purpose of this program was to convert the file format of fMRI images. The neurosurgeon's MR scanner could read images in a certain type of dicom format. Functional images are analyzed in AFNI, and can only be saved in the following formats: .ppm, .jpg, .gif, .tif, .bmp, .eps, .pdf, .snd .png.

Using the program AFNI, it is possible to clearly view activation maps from functional images from each slice of an MRI image. Figure 6.1 below clearly illustrates an image obtained from AFNI in .tif format. This image was obtained from subject # 2 during a finger tapping paradigm. The activation points can clearly be seen.

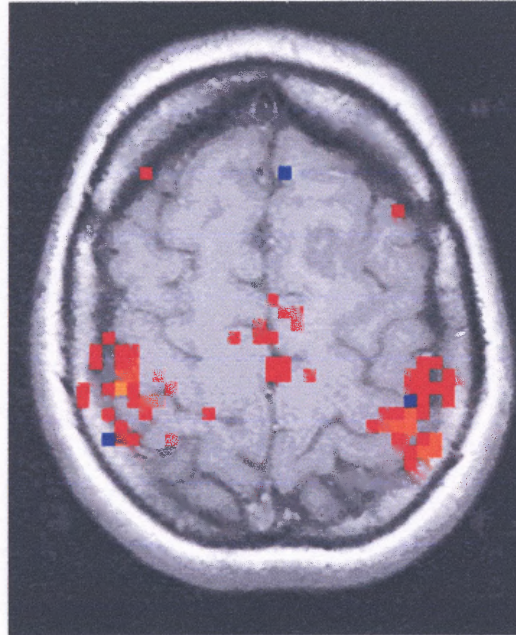


**Figure 6.1** FMRI Image Used in File Conversion Program. Obtained from subject # 2 during a finger tapping paradigm. Image shows that the motor cortex is being activated during this task.

The image depicted in figure 6.1 has certain properties that were obtained using the program Matlab. The image properties are shown in figure 6.2. Images with these properties cannot be read on the surgeon's scanner. The bridge software developed (shown in Appendix C) successfully converts functional images like the image shown in figure 6.1 into a format, which can be read by the surgeon's scanner. The converted image is shown in figure 6.3. The image properties obtained from figure 6.3 are shown in figure 6.4 (page 57).

```

Command Window
FileModDate: '16-Sep-2004 06:45:14'
FileSize: 231396
Format: 'tif'
FormatVersion: []
Width: 240
Height: 320
BitDepth: 24
ColorType: 'truecolor'
FormatSignature: [73 73 42 0]
ByteOrder: 'little-endian'
NewSubfileType: 0
BitsPerSample: [8 8 8]
Compression: 'Uncompressed'
PhotometricInterpretation: 'RGB'
StripOffsets: [8x1 double]
SamplesPerPixel: 3
RowsPerStrip: 44
StripByteCounts: [8x1 double]
XResolution: 100
YResolution: 100
ResolutionUnit: 'Inch'
Colormap: []
PlanarConfiguration: 'Chunky'
TileWidth: []
TileLength: []
TileOffsets: []
TileByteCounts: []
Orientation: 1
FillOrder: 1
GrayResponseUnit: 0.0100
MaxSampleValue: [255 255 255]
MinSampleValue: 0
Thresholding: 1
NewSubFileType: 0
Software: '01/GFS, writer v00.06.02 '

```

**Figure 6.2** Image Properties Obtained from Figure 6.1. Image properties obtained using Matlab function “`imfinfo(filename)`”.



**Figure 6.3** Image Obtained after Conversion to Dicom Format.

The differences between the image obtained from AFNI, and the image obtained by the newly created software are very apparent from figures 6.2 and 6.4. This new Matlab program will allow the neurosurgeon to read functional images during stereotactic brain surgery in real-time. This will allow him to see the activation maps clearly while he is performing surgery. This will result in fewer surgical errors when a neurosurgeon removes a brain tumor.



```

Command Window
FileModDate: '07-Dec-2004 22:41:40'
FileSize: 154618
Format: 'DICOM'
FormatVersion: 3
Width: 240
Height: 320
BitDepth: 16
ColorType: 'grayscale'
SelectedFrames: []
FileStruct: [1x1 struct]
StartOfPixelData: 1010
MetaElementGroupLength: 208
FileMetaInformationVersion: [2x1 double]
MediaStorageSOPClassUID: '1.2.840.10008.5.1.4.1.1.7'
MediaStorageSOPInstanceUID: [1x64 char]
TransferSyntaxUID: '1.2.840.10008.1.2'
ImplementationClassUID: [1x32 char]
ImplementationVersionName: 'MATLAB IPT 3.2'
IdentifyingGroupLength: 174
SOPClassUID: '1.2.840.10008.5.1.4.1.1.7'
SOPInstanceUID: [1x64 char]
StudyDate: '20041207'
StudyTime: '224140'
AccessionNumber: ''
Modality: 'OT'
ConversionType: 'WSD'
ReferringPhysiciansName: [1x1 struct]
PatientGroupLength: 32
PatientsName: [1x1 struct]
PatientID: ''
PatientsBirthDate: ''
PatientsSex: ''
AcquisitionGroupLength: 94
DateOfSecondaryCapture: '20041207'
TimeOfSecondaryCapture: '224140'
SecondaryCaptureDeviceManufacturer: 'The MathWorks'
SecondaryCaptureDeviceManufacturersModelName: 'MATLAB'
SecondaryCaptureDeviceSoftwareVersions: '6.5.0.180913a (R13)'
ImageGroupLength: 176
StudyInstanceUID: [1x64 char]
SeriesInstanceUID: [1x64 char]
StudyID: ''
SeriesNumber: ''
InstanceNumber: ''
PatientOrientation: ''
ImagePresentationGroupLength: 110
SamplesPerPixel: 1
PhotometricInterpretation: 'MONOCHROME2'
Rows: 320
Columns: 240
BitsAllocated: 16
BitsStored: 16
HighBit: 15
PixelRepresentation: 0
SmallestImagePixelValue: 53
LargestImagePixelValue: 255
PixelDataGroupLength: 153608

```

**Figure 6.4** Image Properties Obtained from Figure 6.3. Image properties obtained using Matlab function “dicominfo(filename)”.

## **CHAPTER 7**

### **DISCUSSION**

FMRI, the noninvasive method for analyzing the human brain, was used in this project. FMRI detects changes in blood flow in the brain; however, after a subject is scanned, further analysis must be performed in order to obtain an accurate image. There are many techniques currently being used to reduce noise in these images, such as motion correction, image registration, cross-correlation, t-test, Fourier imaging, etc. These techniques do not have a 100% success rate, and it is not possible to eliminate noise completely in these images; however, a combination of these methods may yield in a more reliable image.

In this study, an innovative method for determining the optimal number of time points required to obtain reliable activation maps was presented. The ultimate goal involved obtaining an accurate functional MR image showing reliable brain activation points which was to be used during stereo-tactic brain surgery.

This new method came one step closer to obtaining an accurate image. When a minimal number of time points are used there is not enough data to successfully obtain accurate results. During long sequential data collection movement is more prevalent which can also alter the results. This results in enough statistical power, and might result in suboptimal estimation due to various confound factors including head motion, habituation, and discomfort. This study clearly showed that an optimal number of time points can be determined to produce the most reliable activation maps.

This method can also be used in various clinical settings including pre-surgical planning. When the location of a brain tumor is determined, it is possible to clearly see the surrounding tissue, and distinguish between healthy and unhealthy tissue. When the optimal number of time points is used to obtain the most accurate image, this image can be used by neurosurgeons. It will result in a more reliable image in detecting the activated region using the least number of time points. This will clearly indicate to the surgeon where to cut during surgery. This method is superior to the previous methods used, because it will eliminate as much noise as possible, and also give the surgeon the correct amount of activated voxels along with their specific location. When a higher number of time points are used, all the activated voxels, are not shown on the image. This will indicate that regions not in white are not being used for certain tasks hence this tissue may be damaged during surgery. The method proposed in this study can be used to better differentiate between healthy and tumor tissue.

This method has many advantages, as well as negative attributes. This can be a computationally expensive method. Depending on the number of time points used while the scan is being performed, the researcher would be required to vary the time points, and physically determine the optimal number from subject to subject. The number 60 was determined to be the optimal number, but this can vary from subject to subject. This number can also vary from task to task. If the subject happens to have very minimal movement during the scan (not possible) then a higher number of time points will yield the best results, however if there is extensive motion throughout the scan a lower number of time points will produce the best results. Sixty time points will result in the best results most of the time, but this may not be the case in every situation.

In addition to this problem, this approach does not take place in real-time, so the results cannot be seen as the subject is being scanned. The images were analyzed when the subject left the facility, and if unreliable activation maps were obtained, the only way to get better results was to call the subject back again. Many times the results obtained were not linear. For example, a certain type of text can elicit a better response in subject # 1 compared to subject # 2. This resulted in more reliable activation maps for subject # 1. This is something that cannot be controlled even if the same text is read to every patient.

The second phase of this project involved the development of a file conversion software, which was successfully completed. The challenge was to address the neurosurgeon's need for functional magnetic resonance images (showing brain activation points) to be used during stereo-tactic brain surgery in real-time. A script file was implemented in the program MATLAB to accomplish this task. The program essentially communicated between surgeon's MR scanner and AFNI (system displaying brain activation points). This program can be used to perform stereo-tactic brain surgery with the use of functional MRI images in real-time. This created the potential of a higher success rate in brain surgeries.

FMRI is a fairly new method to obtain MR images. It is a noninvasive technique to detect changes in blood flow in the brain. As research is conducted in this field new breakthroughs will be developed and more reliable activation maps will be obtained. This project gave researchers and scientists another tool to use when analyzing MR images, by creating a distinct correlation between time points and the reliability of the

collected data. Results from this study can easily be incorporated into analyzing more complex brain activity, as well as in clinical patient populations.

## APPENDIX A

### SCRIPT FILE WRITTEN TO GENERATE MEAN AND STANDARD DEVIATION FOR MOTION CORRECTED DATA

```
%%%%%%%%%%%%%%%%%%%%%%%%%%%%%%%%%%%%%%%%%%%%%%%%%%%%%%%%%%  
%This script was written to calculate values for the mean and standard  
%deviation for the motion corrected data.  
%  
%  
%  
%The script file was written by:  
%Vikram M. Natarajan  
%%10/20/04  
%%%%%%%%%%%%%%%%%%%%%%%%%%%%%%%%%%%%%%%%%%%%%%%%%%%%%%%%%%  
  
%Loads data obtained from AFNI and labels the matrix "Motion"  
Motion=load('MO-FNGR-Run3.1D')  
  
%Defining Yaw and calculating mean and standard deviation of Yaw  
Yaw = Motion(:,1);  
Yaw = [mean(Yaw) std(Yaw)]  
  
%Defining Pitch and calculating mean and standard deviation of Yaw  
Pitch = Motion(:,2);  
Pitch = [mean(Pitch) std(Pitch)]  
  
%Defining Roll and calculating mean and standard deviation of Yaw  
Roll = Motion(:,3);  
Roll = [mean(Roll) std(Roll)]  
  
%Defining AP (Anterior - Posterior) and calculating mean and standard deviation of Yaw  
AP = Motion(:,4);  
AP = [mean(AP) std(AP)]  
  
%Defining RL (Right - Left) and calculating mean and standard deviation of Yaw  
RL = Motion(:,5);  
RL = [mean(RL) std(RL)]  
  
%Defining IS (Inferior - Superior) and calculating mean and standard deviation of Yaw  
IS = Motion(:,6);
```

```
IS = [mean(IS) std(IS)]
```

```
%Organizing data into a 2x3 matrix  
Final = [Yaw; Pitch; Roll; AP; RL; IS]  
clear all
```

## APPENDIX B

### PROGRAM USED TO RECONSTRUCT RAW DATA FROM MRI SCANNER

```
%%This script was written to reconstruct RAW data obtained from the 3T Siemens %MRI
%Scanner into a format that can be read in AFNI.
%
%
%The script file was written by:
%Dr. Bharat Biswal
%University of Medicine and Dentistry of New Jersey
%%
```

```
#!/bin/bash
```

```
# get user input
complete
echo
echo -n "Please Enter Subject Name (file name up to first number): "
read vname
echo -n "Please Enter Highest Run Number: "
read num
```

```
# rename file
```

```
for ((a=1; a<=num; a++))
do
    var1=`echo $vname$a"." $vname$a".0" $(pwd)"/"$vname$a".???.*"`
    var2=`echo $vname$a"." $vname$a".00" $(pwd)"/"$vname$a".??.*"`
    var3=`echo $vname$a"." $vname$a".000" $(pwd)"/"$vname$a".?.*"`

    rename $var1
    rename $var2
    rename $var3

done
```



## APPENDIX C

### SCRIPT FILE WRITTEN TO CONVERT FILE FORMAT

```
%%%%%%%%%%%%%%%%%%%%%%%%%%%%%%%%%%%%%%%%%%%%%%%%%%%%%%%%%%  
%This script file was written to convert the file format of functional MRI  
%images.  
%  
%Converts images from .tif format into a .dcm format.  
%  
%The script file was written by:  
%Vikram M. Natarajan  
%9/30/04  
%%%%%%%%%%%%%%%%%%%%%%%%%%%%%%%%%%%%%%%%%%%%%%%%%%%%%%%%%%  
  
clear all  
  
%Reading fMRI image from AFNI (Shows activation points)  
y=imread('FNGRs4.tif');  
  
%Reading header information from image (Acquired from Siemens 3T Allegra MRI  
%scanner)  
info = dicominfo('VN-BISWAL.MR.HEAD_GENERAL.  
4.0004.2004.9.15.18.2.23.46000.6');  
  
%Scanning AFNI fMRI image to locate activation points  
%Changing color of activation points to white  
for a = 1:1:320;  
    for b = 1:1:240;  
        if y(a,b,1) == 248 | y(a,b,3) ==248  
            y(a,b,1) = 255;  
            y(a,b,2) = 255;  
            y(a,b,3) = 255;  
        end  
    end  
end  
  
%Shows the new image  
imshow(y);  
  
%Converting existing RGB image to grayscale  
y = RGB2gray(y);  
  
%Converting from uint8 to uint16 format
```

```
y1 = uint16(y);
```

```
%Writing image to dicom-format along with the original header information
```

```
dicomwrite(y1, 'vikram.dcm');
```

```
info1 = dicominfo('vikram.dcm');
```

```
Y=dicomread(info1);
```

```
dicomwrite(Y, 'FNGRs4.dcm', info);
```

## REFERENCES

- [1] Peter Armstrong and Martin L. Wastie, *Diagnostic Imaging*, 2nd ed., Oxford: Blackwell Scientific Publications, 1981.
- [2] Ray J. Ballinger, "Relaxation" [online], 1994 [cited March, 5 1996], available from World Wide Web: <<http://www.mritutor.org/mritutor/relax.htm>>.
- [3] Bharat B. Biswal and Paul A. Taylor, "Use of Jackknife Resampling Techniques to Estimate the Confidence Intervals of fMRI Parameters," *Journal of Computer Assisted Tomography*, vol. 25, No. 1, 2001, pp. 113-120.
- [4] Richard B. Buxton, *Introduction to Functional Magnetic Resonance Imaging Principles and Techniques*, 1st ed., New York: Cambridge University Press, 2002.
- [5] Robert W. Cox, *MCW AFNI – User Manual*, Milwaukee: Medical College of Wisconsin, 1996.
- [6] Paul H. Ellenbogen, "Functional MR Imaging (fMRI)- Brain" [online], 2004, available from World Wide Web: <[http://www.radiologyinfo.com/content/functional\\_mr.htm](http://www.radiologyinfo.com/content/functional_mr.htm)>.
- [7] Osamu Hayaishi and Kanji Torizuka, *Biomedical Imaging*, 1st ed., Tokyo: Academic Press Incorporated, 1986.
- [8] Lennart Heimer, *The Human Brain and Spinal Cord*, 1st ed., New York: Springer-Verlag, 1983.
- [9] Eugene R. Jacobs, *Medical Imaging: A Concise Textbook*, 1st ed., New York: IGAKU-SHOIN Medical Publishers Incorporated, 1987.
- [10] Muriel Deutsch Lezak, *Neuropsychological Assessment*, 3rd ed., New York: Oxford University Press, 1995.
- [11] Stuart R. Mackay, *Medical Images and Displays*, 1st ed., New York: John Wiley & Sons, 1984.
- [12] Matlab, ver. 6.5, The Math Works, Incorporated.
- [13] Peter G. Morris, *Nuclear Magnetic Resonance Imaging in Medicine and Biology*, 1st ed., Oxford: Clarendon Press, 1986.
- [14] Fred A. Mettler and Milton J. Guiberteau, *Essentials of Nuclear Medicine Imaging*, 4th ed., Philadelphia: W.B. Saunders Company, 1998.

- [15] Frank H. Netter, *Nervous System*, vol. 1, United States of America: R.R. Donnelley & Sons Company, 1983.
- [16] Leon C. Partain and Ronald R. Price, *Magnetic Resonance Imaging*, vol. 1, Philadelphia: W.B. Saunders Company, 1988.
- [17] Jay W. Pettegrew, *NMR: Principles and Applications to Biomedical Research*, 1st ed., New York: Springer-Verlag, 1990.
- [18] Ricker Polsdorfer, "Surgical Procedures for Brain Tumors" [online], 2003 [cited February 2003], available from World Wide Web: <<http://www.caromont.org/153.cfm>>.
- [19] F. Schmitt and M. K. Stehling, *Echo-Planar Imaging Theory, Technique and Application*, 1st ed., Berlin: Springer-Verlag, 1998.
- [20] Karsten Specht, "Assessment of Reliability in Functional Imaging Studies," *Journal of Magnetic Resonance Imaging*, vol 17, 2003, pp. 463-471.
- [21] David D. Stark and William G. Bradley Jr., *Magnetic Resonance Imaging*, 1st ed., St. Louis: The C.V. Mosby Company, 1988.
- [22] M. T. Vlaardingerboek, and J. A. Boer, *Magnetic Resonance Imaging*, 1st ed., Berlin: Springer, 1996.
- [23] Paul A. Young, *Basic Clinical Neuroanatomy*, 1st ed., Baltimore: Williams & Wilkins, 1997.
- [24] Stuart W. Young, *Magnetic Resonance Imaging: Basic Principles*, 1st ed., New York: Raven Press, 1984.
- [25] Dan S. Heffez, "Diagnoses" [online], 2003, available from World Wide Web: <<http://www.heffezneurosurgical.com/Images/braintumor3.gif>>.
- [26] Michael Schulder, "Functional Image-Guided Surgery for Brain Tumors" [online], 1993, available from World Wide Web: <<http://www.virtualtrials.com/Schulder.cfm>>.
- [27] H. Poinzer, "What the Hands Reveal about the Brain" [online], 1993, available from World Wide Web: <[http://pages.slc.edu/~ebj/IM\\_97/Lecture10/lang\\_areas.gif](http://pages.slc.edu/~ebj/IM_97/Lecture10/lang_areas.gif)>.
- [28] E.M. Purcell and H.C. Torrey, "Pound RV: Resonance absorption by nuclear moments in a solid," *The Physical Review*, vol. 69, no. 37, 1946.